From waste biomass to chemicals and energy via microwave-assisted processes

From waste biomass to chemicals and energy *via* microwave-assisted processes

Emanuela Calcio Gaudino[a], Giancarlo Cravotto[a]*, Maela Manzoli[a], Silvia Tabasso[b]

Formattato: Italiano (Italia)

Abstract

Lignocellulosic waste material represents a considerable renewable feedstock to replace oil refineries with biorefineries. Indeed, all the biomass components can be converted into platform chemicals, bioenergy and materials. However, thermo-chemical and catalytic conventional conversions suffer from certain drawbacks. New technologies such as microwaves have been studied to reduce the process time and the energy consumption leading to an improvement in the product quality and yields. Several beneficial effects of MW over conventional heating due to MW dielectrical interaction with biomass were well documented in this review. Moreover, the use of alternative solvents that strongly interact with MW within biphasic systems could avoid additional upgrading and separation steps. Finally, this review discussed some of the challenges of MW irradiation such as poor dielectric properties of some substrates as well as issues related to large-scale implementation of this technology applied to pyrolysis, hydrothermal conversion and catalytic routes to biofuels, materials and platform chemicals. Waste biomass can represent the benchmark feedstock to develop a circular bioeconomic approach.

1 Introduction

Owing to the strong demand and consumption of fossil sources by the refineries for the production of energy and materials, a new concept of biorefinery has caught up recently. Analogously to an oil refinery, a biorefinery should convert all the components of renewable sources (mainly biomass) to energy and marketable products, through sustainable processes. The aim is to replace fossil fuels with biomass as feedstock in the production of energy and chemicals. Lignocellulosic biomass, such as crops, wood, agricultural and forestry residues, is a major biomass resource and has been recognized as a sustainable feedstock for this purpose. These drivers for bio-fuels and bio-derived chemicals are powering the development of new zero-waste biorefinery technologies. Very generally, (thermo)chemical and/or biochemical routes are usually applied to biomass conversion to bioenergy and high added-value chemicals, according to a biorefinery approach. The former can convert a wide range of biomass types into a broad spectrum of chemicals and materials, and as such, forms the basis of this review, while the biochemical way will be not taken into consideration in this paper. The thermochemical treatment of biomass is conducted at elevated temperatures and typically encompasses two ways: pyrolytic and hydrothermal.[1] The former proceeds under inert atmosphere and with only a limited amount of water, while hydrothermal conditions require significant pressure in the presence of an excess of water, and, often, strong acids. These high temperatures and pressures will accelerate the acid-catalysed hydrolysis of cellulose and hemicellulose, as well as the acid-catalysed degradation of glucose and xylose. Therefore, in this paper, the catalytic route for the conversion of the hydrolysis products into chemicals will be also taken into consideration (Fig.1).

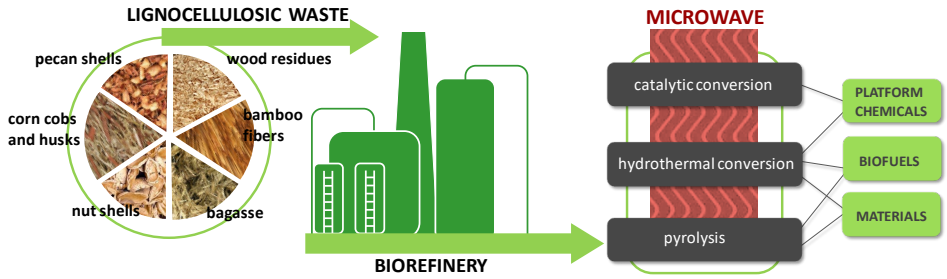

Fig. 1: Schematic path of the biorefinery approach for MW-assisted biomass conversion.

2 Microwave interaction with biomass

One of the drawbacks related to the thermal biomass conversion platforms concerns the heat transfer, limiting the process efficiency. To overcome this limit, microwave-assisted processing of biomass has received significant attention in recent years. In addition, this technology is also capable of improving product quality.[2] Microwaves can penetrate materials and deliver energy, thus heat is generated through the volume of materials (referred to as in-core volumetric heating), instead of conduction and convection occurring through conventional heating. Therefore, microwave heating shows a much higher temperature at the central of the material comparing to the surrounding material, while under conventional heating, the container walls and the outer part of the material are hotter.[3] As a consequence, as microwaves pass through, for example, a piece of biomass, significant temperature gradients may be established between the hot internal regions and the surface of the sample, leading to the centre of the piece being hotter than the outside, where heat dissipates more readily (Fig.2).[4] Furthermore, in the case of lignocellulosic biomass, the effect of MW irradiation at a molecular level leads to a physical disruption of the internal composition of cells, increasing the rate of mass transfer. As a consequence of the inhomogeneity of microwave field and of the microstructure of the biomass, “hot spots” (localized heating leading to much higher temperatures than the bulk).[5] It has been demonstrated that “hot spots” strongly influence the yield and quality of microwave processing products.[6] Microwave heating is usually referred to as “dielectric heating”, as it is generated after the friction of the molecules, owing to the interaction with the electromagnetic field. Therefore, the ability of the materials to be heated by microwaves depends on their ability to absorb and store energy (dielectric constant) and the potential to disperse this energy as heat (dielectric loss). Materials able to strongly interact with microwaves owing to their dielectrical properties are called absorbers.[7] In terms of biomass, the most polar and mobile are the components, the most they will absorb microwaves effectively (thus, for example, amorphous region of cellulose absorbs much better than the crystalline one).[8] Therefore, water is generally the most strongly absorbing species in biomass, but, at increasing temperatures, the water content drops. However, as the reaction proceeds, some absorbent products may be formed (such as, for example, char from pyrolysis). On the other hand, it is possible to further increase the biomass interaction with MW by the addition of external absorbers (as described in section 4.1.1). Transforming electromagnetic energy into thermal energy, microwave-assisted processes are more rapid, affording shorter conversion times than those of conventional heating.

Fig.2: Cross-section of wood after 3 minutes of microwave radiation. Reprinted with permission from M. Miura, H. Kaga, A. Sakurai, T. Kakuchi, K. Takahashi*, J. Anal. Appl. Pyrolysis*, 2004, **71**, 187–199, Copyright 2018, Elsevier.

The unique internal phenomenon associated with microwave energy not only leads to a more efficient energy transfer and heating, but also to a new chemical profile of the products, different from when a conventionally heated biomass processing was carried out at the same apparent temperature. This difference can be ascribed to the non-thermal effects of microwaves,[9] namely, effects that are not correlated with temperature change, due to the interaction of the magnetic field with the biomass components. In particular, it has been demonstrated that at the glass transition temperature of the biomass components, an increasing microwave absorption occurs, owing to the increase in mobility of chain ends.[10] In the case of cellulose, for example, the protons associated with the $–CH_2O(6)H$ group become more accessible, as microwaves could relax or activate the hydrogen bonds at O(6), making them free to rotate and promoting their alignment with the MW field.[11] These groups transfer the microwave energy to the chemical makeup, as they behave as "molecular radiators". Therefore, the interaction of MW with biomass influence the process and the products in two ways: (i) promoting the hydrolysis[12,13] (ii) involving different pyrolytic mechanisms, thus lowering the temperature at which pyrolysis occurs.[14]

3 Microwave-assisted processes for biomass conversion into chemicals

Aiming to guide the emerging research in the production of bio-based chemicals derived from cellulose and hemicellulose, in 2004 the U.S. department of Energy delivered a list of 15 target molecules[15] that includes organic acids (e.g., lactic, succinic, levulinic, fumaric, and itaconic acid) and polyols (e.g., xylitol, glycerol and sorbitol). Bozell and Petersen[16] reviewed this list in 2010 by reducing it into 10 molecules (Fig. 3), but even today the strategy of "platform molecules" aims to explore new technologies for the conversion of bio-derived molecules into all achievable high value-added chemicals. This scope could be achieved through hydrothermal liquefaction of biomass or catalytic conversion of the hydrolysis products.

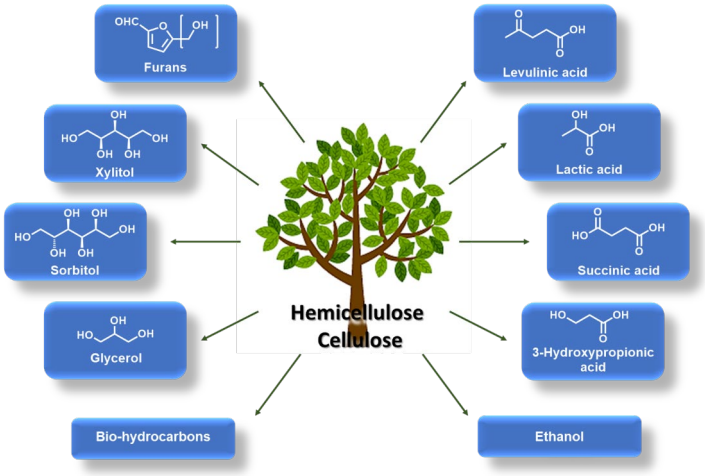

Fig. 3 Bio based chemicals derived from lignocellulose biomass.

3.1 Hydrothermal liquefaction (HTL)

As HTL degradation takes place in water, the first degradation products into small molecules are present in the aqueous fraction. Therefore, the complete characterization of this fraction is mandatory for the detection of valuable products. HTL conditions strongly influence the aqueous products; [17] in particular, the reaction temperature and the residence time are crucial. For example, Liu *et al*. investigated the effect of these parameters on the composition of the aqueous fraction coming from the HTL of rice straw, both under MW and conventional heating (Fig. 4).[18] The temperature strongly influenced the products pattern, but the residence time becomes important when comparing the different technologies. Indeed, a 5 min. MW treatment at 210 °C afforded considerable yields of sugars, while 30 min were required when using conventional heating. In addition, repolymerization and further decomposition reactions were avoided during the mild MW-assisted HTL of rice straw, giving levoglucosan, glucose, xylose, fructose, acetic acid, and formic acid as the main products.

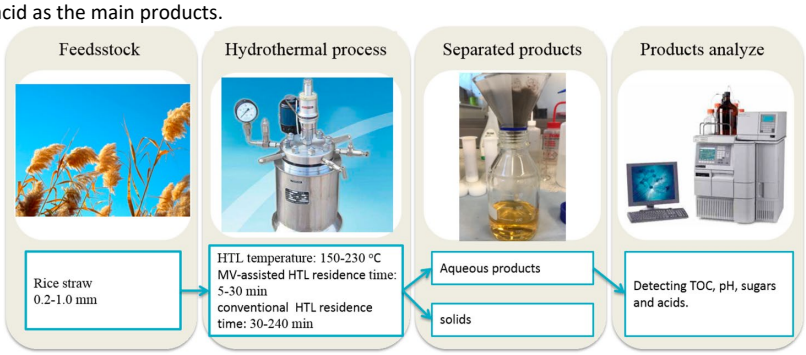

Fig.4: MW-assisted and conventional HTL of rice straw. Reprinted with permission from Liu, Chong; Zhao, Qing; Lin, Yechun; Hu, Yihuai; Wang, Haiyan; Zhang, Guichen, Energy Fuels 2018, **32,** 510−516. Copyright 2018, American Chemical Society.

Besides water, other solvents may be used to promote the liquefaction of biomass into high added-value products. For example, Huang *et al*. reported the acid-catalysed liquefaction of rape straw in methanol under

MW.[19] The chemical reactions included the decomposition of cellulose, hemicellulose and lignin, but the oxidation of hydroxyl groups and methanol esterification were also present. A high content of hydroxyl groups was detected in the methanol fraction at relatively mild conditions (140°C, 15 min.), while a high yield of levulinic ester products was achieved at higher temperatures (180°C, 15 min.). Concerning the energy consumption, higher temperatures led to a higher efficiency, due to MW heating. Recently, many efforts have been focused on the use of wood waste as a raw material to obtain valuable products under mild conditions. With this aim, MW-assisted HTL was compared with conventional heating in the HTL of wood using phenol as the solvent.[20] Besides enhancing the rate of wood liquefaction, MW-heating afforded almost the same chemical components coming from the interaction with phenol than those coming from the conventional liquefaction. The similar substitution pattern with bonded phenol prompts the use of MW as an efficient method to promote the rapid conversion of wood into a bio-polymer precursor.
Recently, Fan *et al*. described a process for the simultaneous production of lignin and oligosaccharides from rapeseed meal, using acetic acid as the catalyst at temperatures ranging from 150 to 210 °C. A gaseous fraction, a liquid one and a solid were obtained in different yields according to the reaction conditions. High purity lignin, unmodified cellulose, hemicellulose and proteins were the main components of the solid fraction, which decreased at increasing temperatures. Humin formation was prevented by acetic acid, which contributed also to the solubilisation of cellulose and hemicellulose. The yield of the liquid fraction was enhanced by higher temperatures and contained mainly oligosaccharides (33-51%) and carboxylic acids (40-62%), with lower amounts of mono/di-saccharides (0–3 C-wt.% and 0–6 C-wt.%). The highest cellulose solubilisation was achieved at 186°C for 2 min. reaction time using of acetic acid 1M. Under these conditions, the lignin content of the solid (85 wt%) was not modified, and a pure saccharide was recovered. [21]

3.2 Catalytic conversion

Toward a practical application, research should “refresh” traditional reaction concepts and intensify efforts to integrate catalytic reaction and new technologies. The routes belonging to the former path might take advantage from new technologies aiming to guarantee environmental friendly processes. The application of MW heating is a fast growing research area, where high reaction rates and selectivity can be achieved together with a significant reduction of the reaction time (often by orders of magnitude) and of energy consumption.[22] In addition, reproducible experiments can be currently carried out, especially thanks to the use of new generation of MW “mono-mode” or “multi-mode” devices that enable a very tight control of reaction parameters. Furthermore, recently flow MW reactors have been developed[23] and could be exploited for biomass conversion in a pilot scale prospective.

Herein, we attempt to provide the state-of-the-art of biomass conversion into some of the most used platform chemicals, under MW assisted catalytic procedures, which is a rapidly developing topic.

3.2.1 Levulinic acid production

It is well documented in literature that during acid catalyzed thermal-hydrolysis of biomass, cellulose and hemicellulose are degraded into hexoses and pentoses (e.g. glucose, xylose, etc.), key intermediates in the further production of various added value products such as furfural (FA), 5-hydroxymethyl furfural (5-HMF), levulinic acid (LevA) and formic acid (FA).[24] Among the various biomass-generated chemicals, LevA , has been considered one of the top building block chemicals which has wide applications in food, medicine, agriculture, cosmetic, and fuel industries. The fundamental mechanism which enables the LevA production from biomass sources is the hydrolysis of cellulose and hemicellulose to carbohydrates, their selective dehydration to 5-HMF and subsequent rehydration into LevA, with a theoretical yield of 64.5% (due to the conjoint formic acid formation). Due to its molecular structure, LevA can be converted into various valuable chemicals.[25] For example, LevA could be hydrogenated into γ-valerolactone (GVL),[26,27]2-methyltetrahydrofuran,[28] valerate esters,[29] 1,4-pentanediol,[30] etc. Meanwhile, different organic acids (e.g., succinic acid and maleic anhydride) could be obtained through LevA oxidation[31] and a plethora of pyrrolidinones could be finally synthesized starting from LevA via reductive amination approach.[32] (Scheme 1). However, the production of LevA is

limited by its ability to corrode most equipment used for its manufacture, and the necessary complexity of the separation equipment.

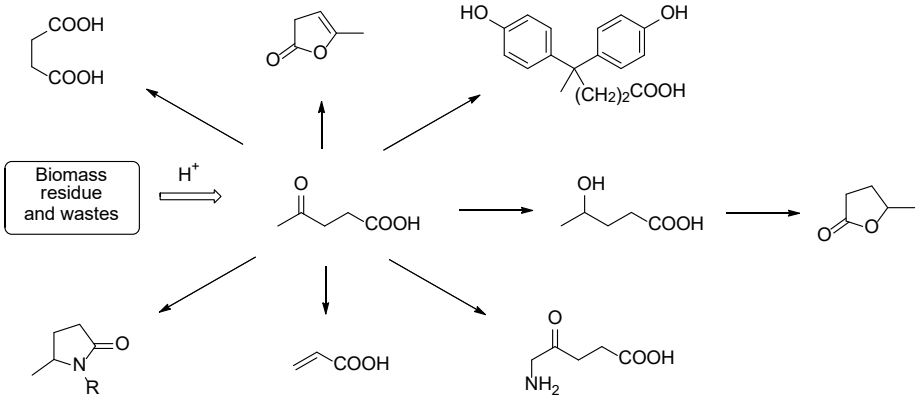

Scheme 1. Selected applications of LevA as a C5-platform molecule.

The inherent chemical complexity of biomass waste makes it a very attractive source to produce value-added chemicals such as LevA. This goal can be achieved by means of sustainable and integrated processes using low environmental impact technologies and efficient energy sources such as MW.

Numerous catalysts have been recently described in literature for the direct biomass hydrolysis and conversion into LevA (trifluoroacetic acid,[33] solid acid catalysts and polyacids including amberlites,[34] zeolites,[35] and many others) but in general, the most common procedure entails the use of mineral acids. Cha and Hanna established that the reactivity order of main mineral acids was HBr > HCl > H_2SO_4 corresponding to the strength of their primary dissociation constants.[36]Among them, volatile acids such as HCl are preferred because they ensure simpler recovery of LevA,[37] although they usually give no more than 7–10 wt% yield in long reaction times. In this context, Tabasso *et al*. (2014)[38] address the requirements for a faster LevA production combining a cost-effective acid catalyst with a MW assisted process (Scheme 2). A suitable lignocellulosic feedstock, the post-harvest tomato plant (PHTP), was used for this purpose. The authors evaluated first the effect of HCl concentration (from 12 to 0.1 M) on MW-assisted biomass conversion into LevA. Although it has recently been reported that low acid concentrations foster the 5-HMF formation, no 5-HMF was detected under MW irradiation at 225°C under HCl concentration ranging from 12 to 0.5 M. However, no LevA was produced from PHTP adopting a HCl concentration lower than 0.1 M. As shown in Table 1, at temperatures lower than 225 °C the selective hydrolysis of biomass carbohydrates into simple monosaccharides (MSC) was favoured. Finally, the optimized PHTP biomass conversion into LevA (63–95% yield) was described at 225°C in only 2 min of MW irradiation in presence of HCl 1 M. These impressive results come from the performance of the MW reactor used that enables fast heating/cooling step and high gas pressure control. Moreover, this protocol proved to be highly versatile since it can selectively give either simple sugars or pure LevA by changing only the reaction temperature.

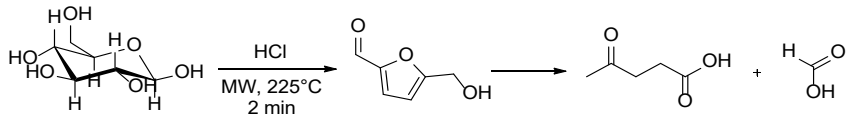

Scheme 2. Conversion of Sugar to LevA and Formic acid.

Table 1. Data for MW assisted conversion of post-harvest tomato plants (PHPT)[a] Reprinted with permission from S. Tabasso, E. Montoneri, D. Carnaroglio, M. Caporaso, G. Cravotto, *Green Chem.*, 2014, **16(1)**, 73. Copyright (2014) Royal Society of Chemistry.

Entry	HCl (mol L^{-1})	T (°C)	Conversion (%)	Yield (%)	
				LA	MS
1	12	225	80	58	0
2	5	225	79	60	0
3	1	225	78	63	0
4	0.5	225	74	51	0
5	0.1	225	67	0	49
6	1	60	30	0	11
7	1	100	30	0	30
8	1	150	62	0	52
9	1	190	81	61	0
10	1	250	80	56	0
11[b]	1	225	73	59	0

[a] Reaction conditions: PHTP/HCl solution = 1/10 (w/V), 2 minutes MW.
[b] PHTP/HCl solution = 1/5 (w/V)

Tabella formattata

Formattato: Allineato al centro, SpazioDopo: 0 pt, Interlinea: singola

In this context, Kumar et al. (2015) [39] recently demonstrated the synergistic effect of $ZnBr_2$ and HCl in the carbohydrate conversion into levulinic acid performing the reaction for the first time in a multimode MW oven (output power 1200 W) under moderate reaction conditions (90°C for 1-6 min) (Scheme 3). MW irradiation of glucose either in the presence of HCl alone or HCl and $ZnBr_2$ together as catalytic system yielded the formation of levulinic acid. But the conversion of glucose to levulinic acid was much faster when both HCl and $ZnBr_2$ were employed together (53 wt% 6 min). To explain these results, the authors hypothesized the *in-situ* generation of HBr from the $ZnBr_2$ and HCl catalytic system that could aid the faster and selective conversion of carbohydrates to levulinic acid. Even Ronen et al. (2013) [40] have previously demonstrated that the Bronsted acid sites are necessary for the selective production of levulinic acid for the conversion of glucose under conventional conditions when ZrP and SnP were exploited. But this new MW assisted method based on the $ZnBr_2$ and HCl combination was particularly important as it involve mild reaction conditions avoiding the formation of degradation products (like humins and carbon residues) usually detected during the catalytic conversion of carboydrates into levulinic acid always performed at higher reaction temperature (150-220 °C) and prolonged reaction time (up to 40 h) (Table 2).

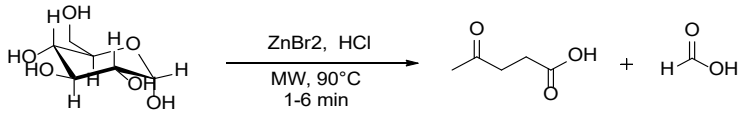

Scheme 3. MW Conversion of glucose to levulinic acid.

Table 2. Strategies for the production of levulinc acid. Adapted with permission from V. B. Kumar, I. N. Pulidindi, A. Gedanken, *RSC Advances*, 2015, **5(15)**, 11043. Copyright (2015) Royal Society of Chemistry.

Feedstock	Catalytic process	Yield
Gelidium amansii	Hydrothermal; H_2SO_4 (3 wt%), 40 h, 180 °C	45.84 wt%
Carbohydrate (glucose, hemicellulose)	Microwave; H_2SO_4, 120 min, 160 °C	69 mol%
Sucrose (0.1 M)	Amberlyst-36, 150 °C, 100 min	65 mM
Glucose, cellulose, cedar	Pretreatment with [EMIM]P at 150 °C, 60 min; hydrolysis with H_2SO_4 (5 wt%) at 220 °C for 2 h	72.9 mol%
Glucose (0.1 M)	H_2SO_4 (1 M), 140 °C, 12 h	60 mol%
Steam exploded rice straw	$S_2O_8^{2-}$–ZrO_2–SiO_2–Sm_2O_3; 200 °C; 10 min, 13.3 wt% of solid acid catalyst	22.8 wt%
Wheat straw	Hydrothermal process; 209 °C; acid catalyst (3.5 wt% of biomass), 37.6 min	19.9 wt%
Glucose	Hydrothermal process; MFI-type zeolite (SiO_2/Al_2O_3 = 30 mol%); 180 °C; 8 h	35.5 wt%
Cicer arietinum, cotton, *Pinus radiata* and sugar cane bagasse	Hydrothermal process, 423 K, 2 h; HCl (1 M)	19–44 wt%

A simple, highly efficient and tunable MW-assisted conversion protocol of seaweed-derived agarose into LevA or 5-HMF according to reaction conditions, is documented by Francavilla *et al.* (2016)[41] (Fig. 5). The reported MW assisted protocol (180 °C, 10 min) features an unprecedented selectivity switch between the production of LevA (64% maximum yield with the addition of 1% sulfuric acid) or HMF (51% maximum yield in without catalyst) starting from agarose in water solution. Moreover, galactose could also be produced as the main product (45–75%) depending on MW temperature and sulfuric acid amount. A plausible reaction mechanism is shown in Scheme 4: the formation of intermediates from agarose hydrolysis is the main critical issue towards LevA or 5-HMF production. These results may pave the way for the selective conversion of seaweed biomass into platform chemicals using an environmental friend protocol.

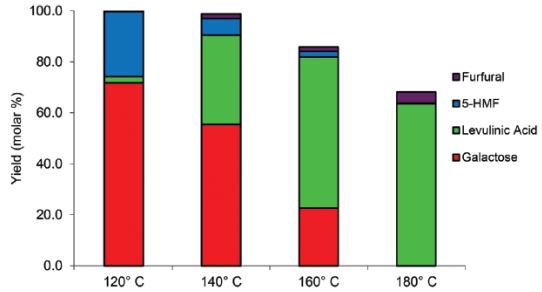

Fig. 5. Product profile obtained in the MW -assisted conversion of agarose in aqueous acid solution (H_2SO_4, 1% v/v) at different temperatures. (Conditions: 50 mg of agarose in 2 mL of aqueous acid solution (H_2SO_4, 1% v/v) in MW at 120 °C, 140 °C, 160 °C and 180 °C, 10 min). Reprinted with permission from M. Francavilla, S. Intini, L. Luchetti, R. Luque, *Green Chem*. 2016, **18(22)**, 5971. Copyright (2016) Royal Society of Chemistry.

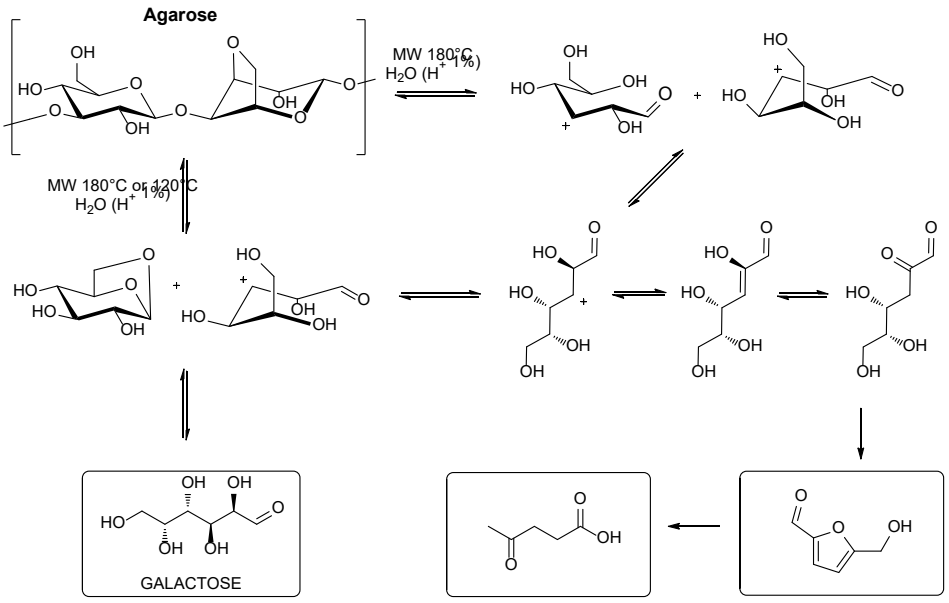

Scheme 4. Proposed reaction mechanism for MW assisted conversion of agarose into LevA 5-HMF and galactose.

Tukas et al (2017)[42] recently demonstrated that cheap and readily available lignocellulosic wastes such as straws, vegetable and fruit peels, shells and husk as well as food wastes produced on large scales (e.g. spent coffee grounds and cooked tea leaves wastes) could be processed as raw materials to produce levulinic acid, a versatile C5-platform chemical. Depending on waste type, when sulfuric acid solution (2 M) was used for conversion, the LevA yields were in the range of 10-25% at 170 °C. Moreover, the reaction time could be significantly reduced to 1/16th when MW technique was applied by means of a multimode reactor (30 min instead of 8 h) without a decrease in product formation. The influence of biomass water content, which could be crucial for drying processes on the levulinic acid formation was investigated revealing that it had no significant effect on the final yields. Thus, the high energy demand pretreatment process can be eliminated from the MW process.

Moreover, the replacement of traditional feedstock with the agro-industrial wastes can bring down the total operating cost of LevA production from (59–75%) to 20–40%. In this context, Maiti et al. (2018)[43] has recently demonstrated the successfully use of agro-industry wastes as a possible sustainable feedstock for LevA production. In particular, they exploited the MW-assisted acid-catalyzed thermal hydrolysis of apple pomace solid wastes (APS) and ultrafiltration sludge (APUS), the brewery liquid waste (BLW) and spent grain (BSG), and the starch industry waste (SIW) as alternative feedstock for LevA production. Two different hydrolysis techniques were compared starting from each dried waste: (a) Brønsted acid catalyzed method by means of an autoclave device, (b) Brønsted acid catalyzed method under MW multiwave digester-working at 1000W. The MW-assisted hydrolysis performed in presence of HCl (2N) and adopting a substrate concentration of 40 g/L enabled a LevA production of 204, 160, 66, 49 and 12 g/kg respectively in only 60 min at 140 °C staring

from BLW, BSG, APS, APUS, and SIW. Based on these preliminary results, BLW and BSG were selected for optimization. Maximum LevA production of 409 and 341 g/kg for BLW and BSG, were finally obtained in only 27.5 min of MW irradiation at 160 °C, in presence of HCl (4.5M), starting from 85 g/L of substrate concentration. The reported results (Table 3) demonstrated the possibility of exploiting brewery wastes as promising substrates for higher production of LevA. The bio-valorization of agroindustry wastes into platform chemicals by means of sustainable technologies could bridge the gap between agro-industry waste production and bio-based economy.

Table 3. Product yields of screened agro-industrial processing wasters using MW assisted homogeneous acid hydrolysis. Reprinted with permission from S. Maiti, G. Gallastegui, G. Suresh, V. L. Pachapur, S. K. Brar, Y. Le Bihan, P. Drogui, G. Buelna, M. Verma, R. Galvez-Cloutier, *Biores. Technol*., 2018, **265**, 471. Copyright (2018) Elsevier.

Feedstock	TRS (g/kg)	Glucose (g/kg)	Xylose (g/kg)	5-HMF (g/kg)	Furfural (g/kg)	LA (g/kg)
BLW	123.10	34.10	ND	7.60	6.50	204.40
BSG	141.20	32.70	ND	8.20	48.20	159.70
APS	258.80	53.90	9.40	6.70	24.30	66.40
APUS	296.80	143.90	ND	12.60	8.40	49.50
SIW	253.30	146.20	ND	35.80	6.10	12.00

3.2.2 Methyl levulinate (MLevA) production

Among the other useful chemicals that can be produced from biomass carbohydrates there are levulinate esters. In particular, methyl levulinate (MLevA) has recently shown potential applications as fuel additive[44] and applied in many other fields, such as organic chemistry, medicine, and cosmetic industry.[45] As alternative to LevA, due to its lower boiling point (about 190 °C), and less corrosive properties MLevA has shown even better performance in term of time and energy consumption in the production and separation processes. Due to the recalcitrant crystalline structure of biomass cellulose, most of the reported studies on MLevA production have exploited model compounds, although the direct conversion of biomass into high quality MLevA is of great interest. In this context, the first example of a selective catalytic conversion of different biomass wastes into MLevA was reported by Feng et al. (2018).[46] The goal of their investigation was to develop a biomass directional liquefaction process exploiting dielectric heating to produce MLevA. In particular, MW assisted biomass methanolysis was investigated in presence of different catalysts including liquid and solid strong acids (i.e., HNO_3, H_2SO_4, HCl or $C_7H_7SO_3H$ and NH_2SO_3H), heteropolyacids ($H_4SiW_{12}O_{40}$ and $H_3PW_{12}O_{40}$), and solid acidic zeolites (HZSM-5 and HBEA). Among others, H_2SO_4 provide the maximum MLevA conversion, while, the lower MLevA yields achieved over HZSM-5 and HBEA was argued by their small pore size (less than 1 nm), which will lead to mass transfer limitations during the directional MW-assisted liquefaction process. Under the optimized condition, the biomass C6 sugars were successfully converted into MLA when H_2SO_4 was used as catalyst in methanol at 180 °C with the highest MLevA yield of approximately 30 wt% for the biomass coming from bamboo (Table 4).

Table 4 Product yields from directional liquefaction using different biomass material. Reprinted with permission from Feng, J. Jiang, C. Y. Hse, Z. Yang, K. Wang, J. Ye, J. Xu, *Sust. Energy & Fuels*, 2018, **2(5)**, 1035. Copyright (2018) Royal Society of Chemistry.

Materials	Conv. (wt%)	MLA yield[b] (wt%)	Furfural yield[c] (wt%)	MLG yield[d] (wt%)
Bamboo	84.11	29.39	18.34	10.22
Eucalyptus	81.25	23.72	19.21	17.32
Poplar	81.14	24.56	14.90	18.45
Pine	80.02	25.67	15.33	19.03
Bagasse	85.02	28.12	17.32	12.27
Straw	79.25	21.67	20.17	17.49

[a] Reaction conditions: biomass materials 2.0 g, methanol 16.0 g, acid catalyst 0.5 g, 180 °C, 40 min. Biomass samples were irradiated for 5 min under 700 W. [b] MLA: methyl levulinate (MLA yields were based on GC analysis with an internal standard method). [c] Furfurals: 5-methoxymethyl furfural and furfural (furfural yields were based on GC analysis with an internal standard method). [d] MLG: methyl pentose glucoside and methyl hexose glycoside (MLG yields were based on HPLC analysis with an external standard method).

This result was even higher than that affordable in aqueous solution for LevA under the same reaction conditions (14 wt% yield). Moreover, the reaction time was significantly reduced by a third when MW irradiation (700 W) was used as a more effective heating method compared to conventional one (40 *vs* 120 min). Different model carbohydrates were finally used by the authors to investigate the possible reaction pathway, finding that the formation of MLA through the MW assisted methanolysis of bamboo followed the sequence: cellulose → methyl glucoside →5-methoxy methyl furfural → MLevA (Scheme 5). The results suggested that directional MW-assisted liquefaction could be an effective method to convert biomass into MLevA.

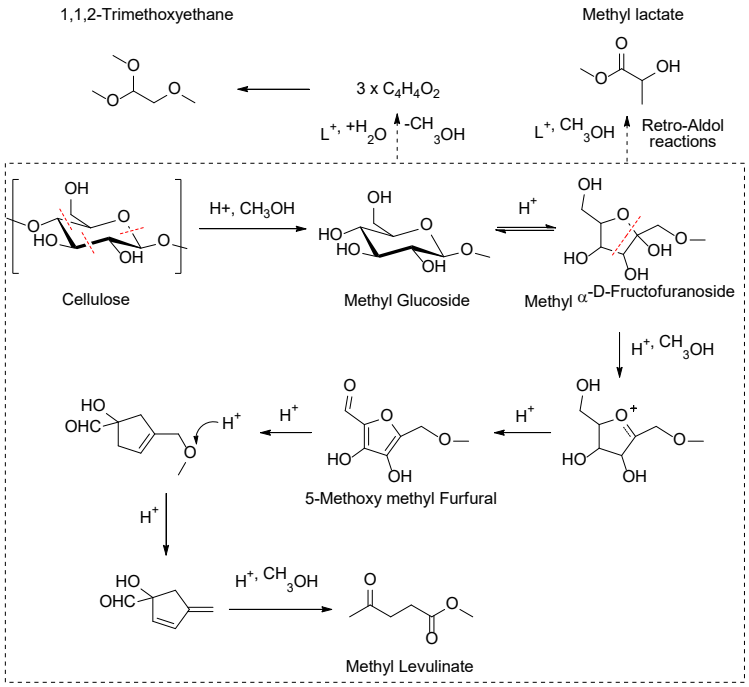

Scheme 5 The proposed liquefaction pathway for the acid-catalyzed conversion of biomass into MLevA in methanol.

3.2.3 Lactic- and Glycolic-Acid production

Among others biomass derived high value-added products, lactic acid (LA) plays an important role as commodity chemical widely exploited in food processing as well as in cosmetic and pharmaceutical industries. LA is used to prepare *inter alia* 1,2-propanediol,[47]green solvents such as ethyl lactate,[48] and biodegradable plastics.[49] Furthermore, to improve the polylactic acid (PLA) properties, some LA copolymers (PLGA) have been synthesized starting from glycolic acid (GA) through direct polycondensation and ring opening polymerization. Due to their high biocompatibility and biodegradability PLA and PLGA co-polymers have found several applications in medical fields.[50] LA is typically produced via monosaccharide fermentation,[51] nevertheless this biological approach does not enable the direct conversion of lignocellulose biomass into monosaccharides without a pretreatment step. Therefore, in the last few years the development of sustainable chemical processes for fast and cost-effective LA production has grown as one of the hottest research topics. In this context, Carnaroglio et al. (2015)[52] entered a fast protocol fully driven by MW irradiation for lignocellulosic waste valorization over two steps: the former conversion of cellulose and PHTP into LA and GA and the use of these high value-added chemicals for the subsequent production of bio-based co-polymers. Using a dilute catalyst solution of $Pb(NO_3)_3$ (35 mm) and working at 220 °C in a batch pressurized (3MPa) MW system, they established a selective protocol which gives in only 2 min (960 W), LA and GA at high conversion, from both cellulose (97%) and PHTP (50%) (Fig. 6). This method is able to produce LA and GA along two different proposed reaction pathways; C2– C3 or C3–C4 retro-aldol reactions (Scheme 6).

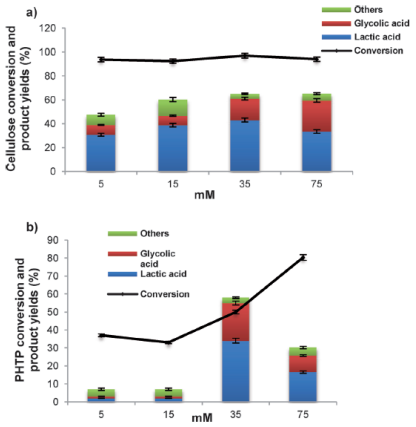

Fig. 6. Effect of different catalyst concentration on the MW assisted conversion of milled cellulose (a) and PHTP (b). Reaction conditions: ball milled cellulose/PHTP (500 mg) 220 °C, 2 min, N2(3 MPa); data from three replications; others: mainly levulinic acid. Reprinted with permission from D. Carnaroglio, S. Tabasso, B. Kwasek, D. Bogdal, E. Calcio Gaudino, G. Cravotto, *ChemSusChem* 2015, **8(8)**, 1342. Copyright (2015) Wiley.

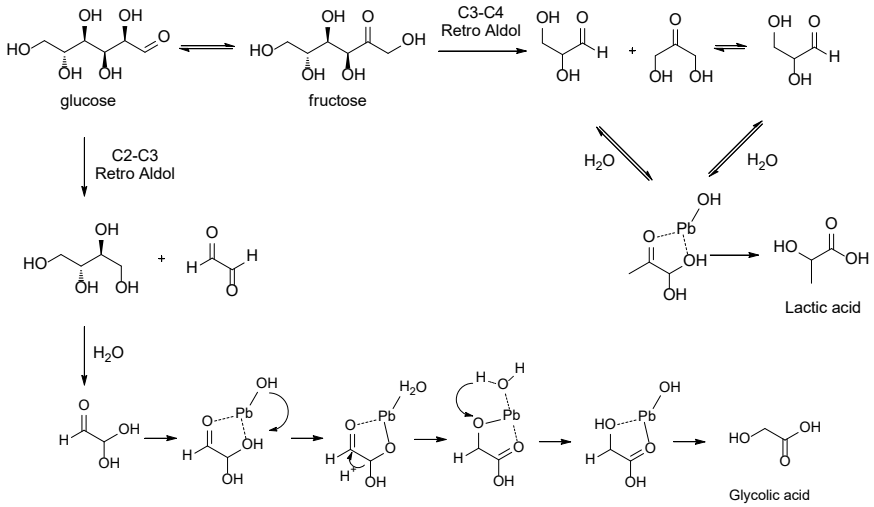

Scheme 6. Proposed reaction pathway for the conversion of cellulose into LA and GA, as catalysed by Pb^{II} in water.

In addition, the optimized MW batch protocol for LA and GA production has been redesigned and converted into a continuous process by means of a MW tubular flow reactor in which conversions and yields were maintained (working at 220 °C, 3 MPa and 18 mL/min), increasing process productivity and lowering energy consumption (0.55 kWh). The so obtained LA and GA mixtures, representing a good starting material for the production of bio-based PLA and PLGA oligomers, were directly poly-condensed under MW irradiation. Impressive results (Table 5) were described under solvent and catalyst free conditions (130 °C, 3h) by means

of a rotavap-like MW reactor working under vacuum (70 mbar). MW- undoubtedly could play a crucial role in the design of sustainable procedures for biomass valorization also on industrial scale by means of flow MW assisted process. Recently, a new MW heated extruder was applied in PLA synthesis by by the Fraunhofer ICT and Mugge.[53]

Table 5. MW assisted direct polycondensation of LA and GA.[(a)] Reprinted with permission from D. Carnaroglio, S. Tabasso, B. Kwasek, D. Bogdal, E. Calcio Gaudino, G. Cravotto, *ChemSusChem* 2015, **8(8)**, 1342. Copyright (2015) Wiley.

Entry	Feed [mol%] LA/GA	Yield [%]	Polymer composition LA/GA[(b)]	M_n[(c)]	M_w/M_n[(c)]	T_d [°C][(d)]
1	100:0	80	100:0	2229	1.53	362
2	50:50	75	53:47	2923	1.47	365
3	70:30	77	69:31	2510	2.00	359

[a] 130 °C, 3 h, 70 mbar. [b] Estimated from the integral height of hydrogen in ^{1}H NMR spectra. [c] Determined by GPC analysis. [d] Determined by TGA.

3.2.4 Furfural and HMF production

Furfural is an attractive platform molecule identified as one of the top value-added chemicals derived from biomass.[54] It is mainly produced from hemicelluloses, the second polysaccharide most abundant in nature, composing about 20% - 35% of lignocellulosic biomass. Hemicellulosic sugars could be reconverted by various hydrothermal processes into different added-value chemicals (such as xylitol, lactic acid ecc.) among which furfural is worth of note as multifunctional bio-derived product: it is employed as precursor for many furan-based products which found high demand in plastic, food, agricultural and pharmaceutical industries.[5556] In particular, furfuryl alcohol, that is the most important furfural derivative, is widely used as a basic component for furan resins production.[57] Furfural is generally produced following a one or two stage process based on the acidic hydrolysis and subsequent dehydration of pentoses (mainly xylose) that composed hemicellulose (Scheme 7).[58] In the one-stage technology, pentosanes are hydrolyzed into xylose and dehydrated into furfural within the same reactor. This process generally gives low furfural yield (0.7–3.3 wt%), and the solid residue can be used only as a source of fuel. In the two-stage process, hydrolysis of pentoses occurs under mild conditions, followed by the dehydration of xylose into furfural in two different reactors. The advantage of the two-stage technology is the higher furfural yield compared to one stage process. Moreover, the recovered solid residue from two stage process is less degraded and can be exploited for conversion to other added value chemicals via fermentation (phenols, ethanol, etc.). The drawbacks of the current furfural production on industrial scale are the processes with low yields, and the corrosive and non-environmental catalysts are being used in the processes.

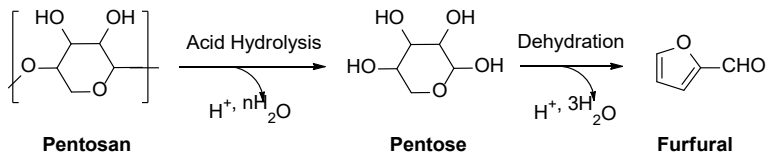

Scheme 7. Acidic hydrolysis of pentosan followed by dehydration to form furfural.

In this context, Sánchez et al. (2013)[59] reported a study focused on the MW assisted hemicellulosic monomers conversion into furfural testing different acid catalysts. In this work, the xylans rich liquors obtained from corn cobs autohydrolysis performed at 180 °C in a Parr device (30 min with a solid:liquid ratio of 1:8) were treated with or without HCl and H_2SO_4 acid catalysts, in order to obtain the maximum furfural production under MW irradiation. The results displayed that the furfural production was strongly influenced by catalyst concentration, and by reaction time and temperature (Fig. 4). The use of acidic catalyst strongly enhanced the furfural production from corn crobs liquors. Up to 37.06% of furfural was achieved (respect to the total hemicelluloses present in raw materials) at intermediate value of temperature (180 °C, 300 W), intermediate value of HCl concentration (2% (v/v)) and highest reaction time (5 min). In addition to furfural, high concentrations of other final degradation products like acetic acid or formic acid were obtained (5.91 g/L of acetic acid and 5.32 g/L of formic acid). Moreover, high xylose concentrations have been noticed at low factor values during MW irradiation, so this technology has proven to be good convert oligomers (contained in corn crob autohydrolysis liquors) into monomers. Finally, it can be concluded that the use of MW technique is suitable to quickly produce furfural from biomass.

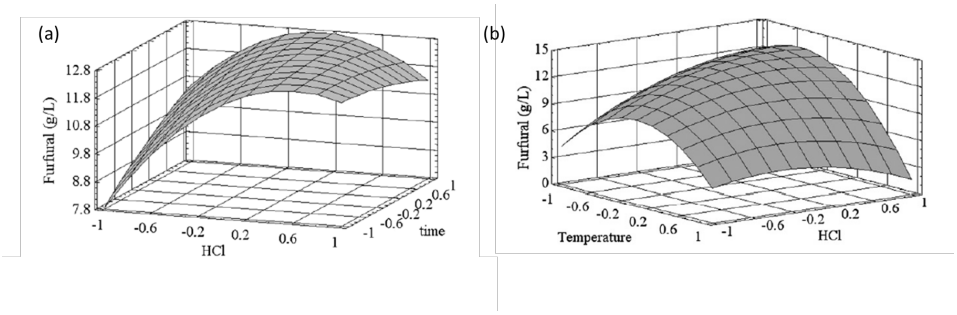

Fig. 4. **a)** Variation of furfural concentration (g/L) with the HCl concentration (normalized) and the time of reaction (normalized) at the central temperature point. **b)** Variation of furfural concentration (g/L) with the HCl concentration (normalized) and the temperature of reaction (normalized) at the central time point. Adapted with permission from C. Sanchez, L. Serrano, M. A. Andres, J. Labidi, *Ind. Crops and Prod.*, 2013, **42**, 513. Copyright (2013) Elsevier.

As mentioned before, pentoses coming from renewable resource can be efficiently converted into furfural. In this context, through a greener synthetic methodology based on MW irradiation, Vaz Jr. & Donate (2015)[60] demonstrated the optimum conversion of D-xylose into furfural in aqueous medium (Scheme 8). The highest furfural yield (64%) was described in presence of HCl (4 mg/mL) when the D-xylose was treated under MW irradiation at 200 °C (400 W) for 10 min, with 95% of D-xylose conversion.

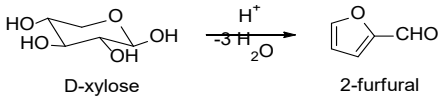

Scheme 8. Conversion of D-xylose into 2-furfural.

MW technology lead to different advantages compared to conventional D-xylose conversion. The authors stated that reaction mixture was rapidly heated to reaction temperature and subsequently quickly cooled down to room temperature, which is beneficial for reaction yields, since it was found that starting material and product are not so stable at elevated temperatures. On the other hand, also the disadvantages of this

MW assisted procedure were listed: the reactions could not be run in parallel, only in a sequential fashion, and this limited the number of achievable results and the potential process scale up. These inconveniences can be solved by adopting new generation of MW devices that enable parallel reactions or flow MW assisted processes.[61]

The hydrothermal conversion of giant reed (*Arundo donax* L.) to furfural and LevA was investigated in presence of dilute hydrochloric acid (1.68 wt%) by Antonetti et al. (2015)[62] (Scheme 9). From an industrial point of view, giant reed biomass is of great interest, because of its high content of cellulose and hemicellulose to be converted in high value products. The catalytic performance was investigated under MW (MW) irradiation (140-190 °C-300 W), enabling significant savings in terms of process energy and time. Hydrolysis time and temperature were carefully optimized; indeed, for FA formation milder reaction conditions were required, whereas for LevA more severe ones. The promising results demonstrate that giant reed could represent a very interesting candidate for high simultaneous production of FA and LevA under MW irradiation in presence of dilute acid, with 70 and 90% yields respectively of theoretical ones (Fig. 7). It is as well interesting to highlight that the best optimized FA and LA yields reached in this study using MW irradiation were higher, when compared with the data reported for conventional heating in the literature.

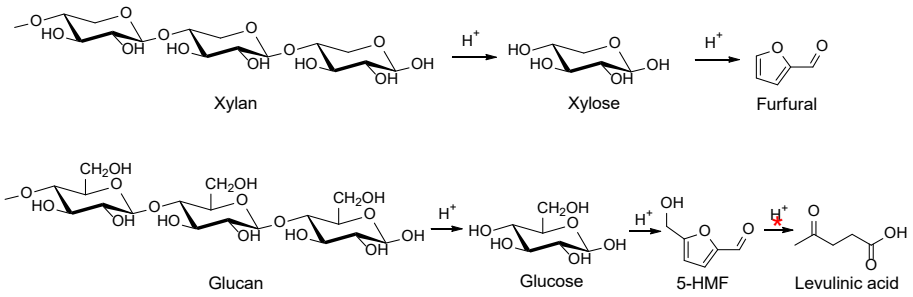

Scheme 9. Synthesis of Furfural and Levulinic acid in the presence of HCl catalyst from giant reed.

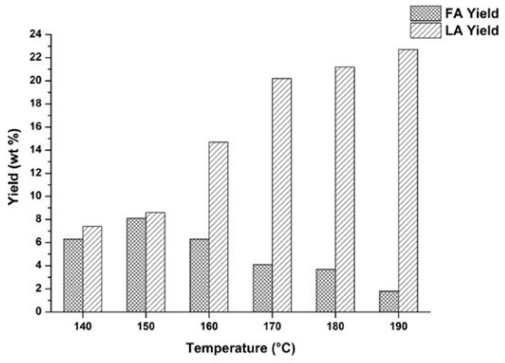

Fig. 7. Optimization of giant reed hydrolysis in a MW reactor: yield in furfural and levulinic acid as function of temperature. Conditions for furfural synthesis: 0.35g giant reed, 5.00 g H2O, HCl concentration: 1.68 wt%. Hydrolysis time: 15 min. Conditions for levulinic acid synthesis: 1.63 g giant reed, 23.33 g H2O, HCl concentration: 1.68 wt%. Hydrolysis time: 20 min.

Another example of MW assisted hydrothermal treatment of pentose rich corncob for furfural production was recently reported by Ren et al. (2016)[63] exploiting $SnCl_4$ catalyst (Scheme 10). The highest furfural yield of around 10 wt% (based on dried biomass weight) was reached for this one step MW assisted process performed at 190 °C (600 W, 50 min) using a 1% of $SnCl_4$ (based on dried corncob weight) and a solid: liquor ratio of 1:20. $SnCl_4$ could effectively cause the release of polysaccharides (xylan and cellulose) from the corncob cell wall and their hydrolysis in the aqueous system under the applied MW condition. Subsequently, the selective dehydration of pentose into furfural occurred under the function of Sn^{4+}, colloidal SnO_2x H_2O and H^+ as the hydrolysis product of $SnCl_4$.

$$Sn^{4+} + (x+2)\ H_2O \Leftrightarrow SnO_2 \cdot xH_2O + 4H^+$$

The recovered biomass residue was finally characterized by XRD, SEM, and FTIR. The results confirmed that the cell wall structure of treated corncob was fairly destroyed under $SnCl_4$ activity during the MW irradiation, and most of the released hemicelluloses (96%) entered the hydrolysate as hemicellulose-derived sugars that were simultaneous dehydrated to furfural. During the same MW assisted process a little amount of HMF coming from hexoses present into the hydrolysate was also detected. As the furfural yield was much higher compared to that of HMF (10 *vs* 0.7 wt% respectively) this proves once again the fact that $SnCl_4$ had high selectivity for furfural production (Fig. 8). Hence, the combined use of MW technology with $SnCl_4$ catalysts shows a promising approach to the sustainable conversion of renewable lignocellulosic biomass into furfural.

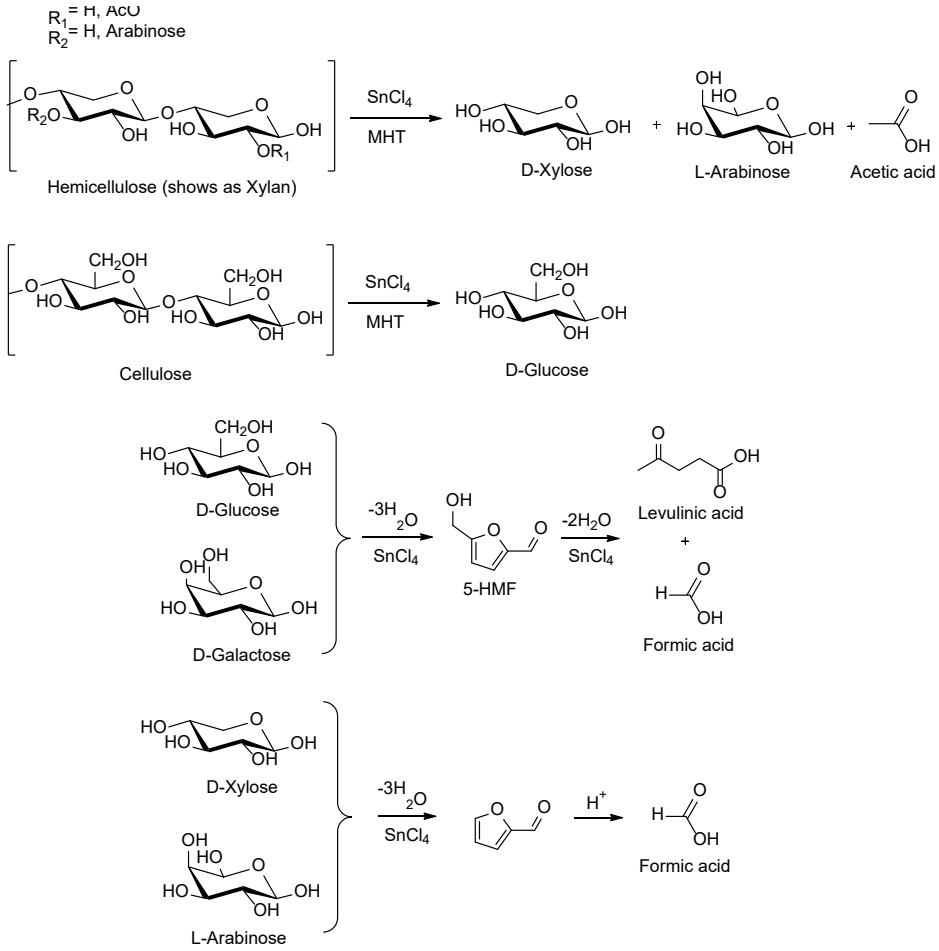

Scheme 10. Possible reaction pathway for the conversion of corn cob carbohydrate into furfural.

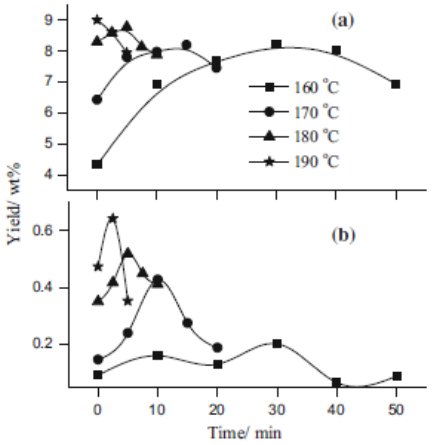

Fig. 1 Effect of reaction temperature and time on furfural and HMF yields. **a** Furfural, **b** HMF

Fig. 8. Effect of reaction temperature and time on furfural and HMF yields. (a) Furfural, (b) HMF. Reprinted with permission from J. Ren, W. Wang, Y. Yan, A. Deng, Q. Chen, L. Zhao, *Cellulose*, 2016, **23**(3), 1649. Copyright (2016) Springer Nature.

Although many studies [64] on pure carbohydrates and lignocellulosic biomass conversion to furfural have been performed under conventional conditions in presence of various solid catalysts and metal halides, Yemiş and Mazza (2017) [65] recently reported the first example of MW assisted one pot catalytic conversion of biomass (straw), xylan, and xylose. Four different solid catalysts (i.e., Amberlyst ®-36, Amberlyst ®-15, Nafion ®-NR50, and DOWEX 50WX8-200) and various metal halides (such as $FeCl_3$, $AlCl_3$, $CaCl_2$, and NaCl) were tested for the MW assisted production of furfural in a single-phase aqueous system. A substrate: liquid ratio of 1:15 and a catalytic loading of 10% (w/w) was adopted at 180 °C for 20 min of MW irradiation. For the conversion of xylose, the Amberlyst- 36 wet was the most efficient heterogeneous catalyst at 180 °C, enabling a 25% of furfural yield in batch mode. However, for the conversion of xylan under the same MW reaction conditions, only 1% furfural yield was reported in presence of the same catalyst. This low furfural yields revealed that xylan was not successfully hydrolyzed into sugars using the solid Amberlyst catalyst under the reported MW conditions. Among the 14 metal halides screened, $FeCl_3$ showed the highest activity for the MW-assisted hydrothermal conversion of straws furnishing different furfural yields (35.3, 41.6, and 65.3%) depending on the starting biomass (wheat straw, triticale straw, or flax shives respectively). Moreover, all the tested metal halides could catalyze the xylose dehydration, but the cation type plays a crucial rule for the formation of furfural in aqueous medium in the reported MW-assisted process. Fe^{3+} was the most effective cation for xylan and xylose conversion furnishing a furfural yield of 26.12% and 27.91% respectively. Previously, Liu et al. (2009)[66] demonstrated that Fe^{3+} cations exhibited strong catalytic activity during the hemicellulose and cellulose hydrolysis of corn stover in aqueous medium. These results indicated that $FeCl_3$ could be applied for hydrothermal treatment of biomass leading to both biomass saccharification or furfural production tailoring ad hoc the MW conditions.

As previously reported furfural industrial production is currently carried out in batch or continuous processes by using strong mineral acid such as HCl or H_2SO_4 starting from pentosane rich lignocellulosic biomass. However, these mineral acids are responsible for serious safety problems, such as corrosion, and even

separation issues have to been addressed when reaction were performed in monophasic systems (water only). In this case the product requires a progressively distillation during the process in order to avoid the formation of black insoluble carbonaceous material named humins. Moreover, furfural recovery from aqueous phase with hydrophobic solvents (such as toluene, nitrotoluene or methylisobutylketone (MIBK)) is always required after the production step leading to an increase in its costs. Biphasic systems could be valid alternatives to obviate these problems. In this context, De Oliveira Vigieret al. (2012)[67] reported earlier a strategy based on biphasic system made of choline chloride (ChCl), and MIBK to produce 5-hydroxymethylfurfural (HMF) under conventional heating. On the other hand, Sun *et al.* (2015)[68] reported the MW assisted conversion of lignocellulosic biomass into 5-HMF in a biphasic H_2O/THF. Starting from bamboo fiber a 50% of 5-HMF yield was achieved exploiting NH_2SO_3H as solid acid catalyst under MW irradiation at 180◦C for 40 min (Fig. 9a). Moreover, the 5-HMF yield could increase significantly if NaCl was added to the biphasic system. NaCl could not only effectively increase the distribution coefficient of 5- HMF between organic and water phase, but also preventing its further conversion to LevA. NH_2SO_3H offered the satisfactory catalytic activity to convert bamboo fiber to HMF due to its relative special structures. Indeed, NH_2SO_3H presents a dual-catalytic functionality due to its tautomeric structure: a Bronsted acid group and a Lewis acid site, which could accelerate the degradation of bio-polymer and subsequent dehydration of the resulting monosaccharides to downstream products. In addition, the MW assisted conversion of some other lignocellulosic biomass such as polar wood powder, pine wood powder, and cotton proved the efficacy of this water/THF biphasic system over NH_2SO_3H catalyst (Fig. 9b).

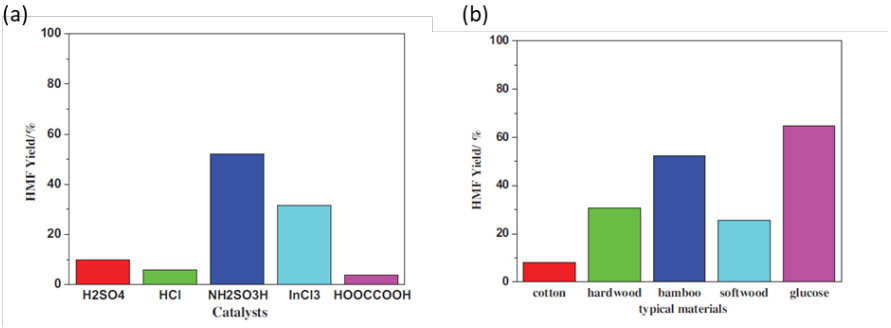

Fig. 9. (a)5-HMF production from bamboo fiber degradation catalyzed by different acidic catalyst (**b**) Effect of different biomass material on the production of 5-HMF. (Condition: lignocellulosic biomass (1.25 mmol), NaCl (1.75 g), catalyst (0.5 mmol), H_2O/THF (1:3 v/v), 180 °C, 40 min. Adapted with permission from J. Sun, X. Yuan, Y. Shen, Y. Yi, B. Wang, F. Xu, R. Sun, *Ind. Crops Prod*., 2015, **70**, 266. Copyright (2015) Elsevier.

However, even more eco-friendly solvents such as cyclopentylmethylether (CPME), were recently documented for furfural recovery from water after MW assisted pentosane conversion. [69] In this context Delbecq *et al.* (2016)[70] reported first the use of a biphasic water- CPME system (1:3 v/v) for the D-xylose dehydration and direct transformation of xylan and rice husk into furfural under MW irradiation exploiting a coupled betaine-formic acid catalytic system. Highest furfural yields were described for pentoses and polysaccharides (80% and 76% respectively) at 170◦C under 1 h of MW irradiation (W) in presence of betaine-formic acid combined catalytic system (pH range 1.9 - 2.3) (Fig. 10). Biphasic system was a suitable choice especially due to the strong stability of CPME in presence of acidic conditions. However, without addition of zwitterionic betaine, the acidity of the reaction mixtures grows, and less amount of furfural was recovered starting from D-xylose (53% yield). This was owed to the formation of by-products generated by the resinification of furfural promoted by the strong acidity of reaction medium. On the other hand, betaine

should promote the furfural production when coupled with formic acid, as it is responsible of intermediate isomerization of xylose into xylulose, a more sensitive species to dehydration step in acidic condition.

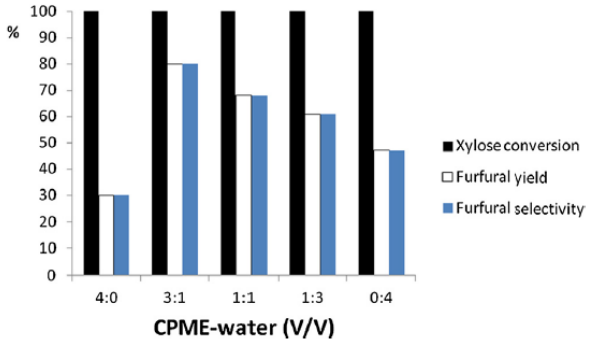

Fig. 10 Effect of the water to CPME phase ratio (v/v) on the furfural production. Reaction conditions: D-xylose (150 mg), betaine (0.07 g), HCOOH (0.25 g), water-CPME (4 mL), MW, 170 °C, 1 h. Reprinted with permission from F. Delbecq, Y. Wang, C. Len, *J. Mol. Catal. A: Chem*., 2016, **423**, 520. Copyright (2016) Elsevier.

The final purpose of this investigation was focused on transferring the optimized MW assisted procedure for the furfural production starting from xilose and xilans to the direct production of furfural starting from rice husk, a rich biomass. Under the described biphasic MW-assisted reaction the target furfural was achieved (6% yield) at 190 °C starting from dried rice husk in presence of betaine / formic acid catalytic system. It could be interesting, as a next step of this process, to check if it be transposed to hexoses and cellulose to produce 5-HMF as the main target compound. To improve the selectivity toward furfural, other biphasic media combining for example water and γ-valerolactone (GVL) were tested at low xylose concentration (below 50 wt%).[71] Even if furfural yields up to 70% were reported in these cases, at higher xylose concentration, these processes suffer from degradation of xylose to resinous compounds, leading to a low furfural yields. Being able to increase the concentration of furfural, while preserving the selectivity of the reaction is of extreme interest as regards the industrialization of this process, but it still remains a crucial scientific question.[72] ChCl, as relatively cheap and biodegradable compound that can form deep eutectic mixture with carbohydrates (DES),[73] has recently been widely exploited for lignocellulose fractionation. More recently Jang et al (2018)[74] deepened the beneficial use of a biphasic water/ChCl: MIBK system in highly concentrated (up to 50%) xylose conversion into furfural (Fig. 11) under conventional heating.

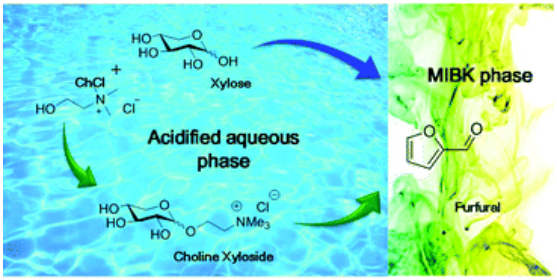

Fig. 11 Unveiling the role of ChCl in furfural synthesis from highly concentrated feeds of xylose. Reprinted with permission from S. Jiang, C. Verrier, M. Ahmar, J. Lai, C. Ma, E. Muller, Y. Queneau, M. Pera-Titus, F.

In presence of this water biphasic system a relatively high production of furfural was described (75% yield) at 120 °C in 4 h. Hence, it was suspected by the authors that a chemical reaction between xylose and ChCl occurred. Fischer glycosylation of xylose with ChCl could be the rational elucidation of these results never observed at lower xylose concentration. In presence of ChCl, the formation of choline xyloside could be followed by 2-OH protonation. This intermediate can undergo ring contraction to form an oxonium-ion still incorporating the choline moiety. This intermediate is then readily hydrolyzed in aqueous media to generate the C-1 aldehyde releasing the ChCl (Scheme 11). The formation of a choline xyloside intermediate was finally documented, proving also its higher reactivity in furfural formation with respect to xylose. These results are extremely fascinating as ChCl due to its polar nature could be successfully applied for even more sustainable xylose conversion to furfural under non-conventional heating by means of MW irradiation.

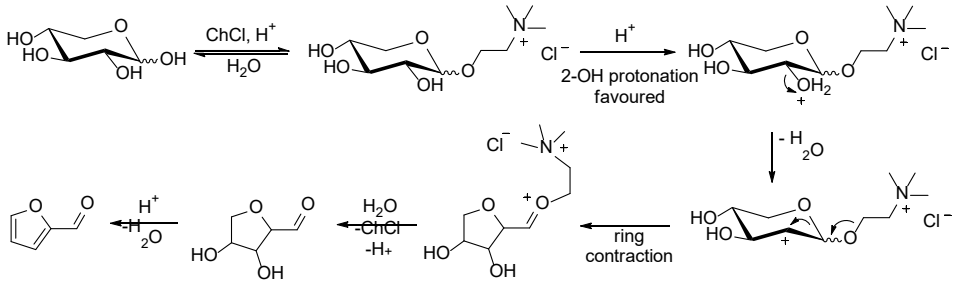

Scheme 11. Proposed mechanism for xylose dehydration to furfural through the formation of choline xyloside and 2-OH protonation.

A representative example of correlation study between the dipole moment of green solvents used and the yield of 5-HMF coming from a MW assisted conversion of bread waste over $SnCl_4$ MW was recently reported by YU et al. (2018)[75].The PC/H_2O and GVL/H_2O systems successfully suppressed the hydrolysis of Sn^{4+} to inactive colloidal SnO_2 particles, which evidently occurred in acetone and water (as revealed by XRD analysis). Moreover, a positive correlation between the dipole moment of green solvents used and the yield of 5-HMF coming from MW assisted waste conversion was documented (Fig. 12). In addition to the improved MW absorption, the greater dipole moment of solvent used causes a stronger solvent strength as a ligand for Sn^{4+} coordination, thus suppressing the metal hydrolysis into the inactive SnO_2. This corroborates a recent investigation on product yields correlation with the extent of dipolar moment in cellulose conversion.[76] This study provides insight into the multiple roles of green solvents pointing out their interplay with catalysts and MW irradiation to reach high conversion of biomass waste.

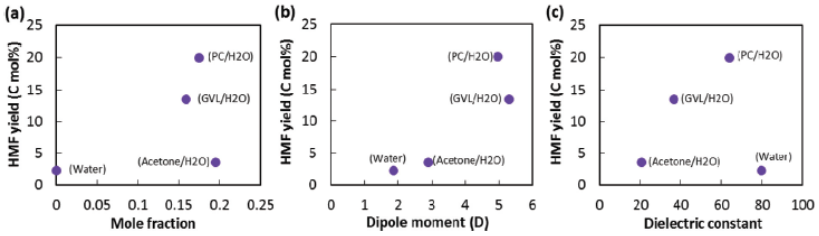

Fig. 12 Correlation between 5-HMF yields from bread waste conversion and (a) mole fraction of organic co-solvent in the binary mixture, (b) dipole moment of the organic co-solvent, and (c) dielectric costant of the organic co-solvent, respectively (conditions: 5 wt/v% susbtrate in solvent mixture (1:1 v/v) or water at 120 °C for 10 min; yield = product $_{Cmol}$/substrate$_{Cmol}$ X 100%). With permission from I. K. M. Yu, D. C. W. Tsang, A. C. K. Yip, A. J. Hunt, J. Sherwood, J. Shang, H. Song, Y. S. Ok, C. S. Poon, *Green Chem.*, 2018, **20(9)**, 2064. Copyright (2018) The Royal Society of Chemistry.

A cascade MW-assisted circular process has been recently developed by Tabasso *et al*. (2016)[77] for the extraction of lignin from PHTP by mean of green GVL produced and regenerated within the same process (Fig. 13). GVL is commonly synthesized from LevA via hydrogenation to 4-hydroxypentanoic acid, which spontaneously condensates to GVL. In this work, the acidic GVL/ aqueous solution (1:1 with HCl 1M) used for PHTP valorization enabled the complete solubilization of biomass deconstruction products after MW irradiation at 225 °C (1500 W) for 2 min and the simple recovery of lignin by simple precipitation with NaCl solution. In addition, the MW-assisted hydrogenation of the obtained LA to GVL in presence of Pd/C (10 wt%) performed at 150 °C (4 h) eliminates the need for a separation step, as GVL is together solvent and product. The remarkable features of this method are: (1) a one-step flash-treatment for both lignin solubilization and conversion of cellulose to LA step; (2) the absence of a purification step for LevA recovery; (3) the double role of GVL (solvent and product) ready to be recycled. This process complies with the six principles of green extraction. This method for lignin extraction may well lead to an upgrade in the subsequent lignin valorization processes in a circular economy perspective.

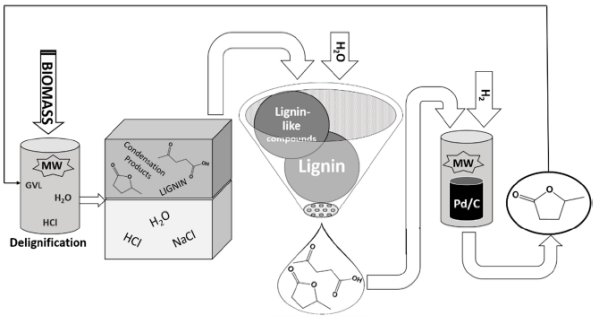

Fig. 13. Scheme of the cascade process for the extraction of lignin from PHTP and GVL production.

4 Microwave-assisted processes for biomass conversion into bioenergy

The thermochemical conversion of biomass leads to the production of liquid, solid and gaseous products similar to those from the oil and gas industry, that can be directly integrated into the existing petroleum

infrastructure. According to the conditions, different products of different quality can be obtained, but, in principles, all the three fractions can be used for bioenergy production (in the form of liquid biofuel, solid fuel and gases for heat and electricity). The main thermochemical processes involved in bioenergy production from biomass are the pyrolytic and the hydrothermal ones.

4.1 Pyrolysis

Pyrolysis is the thermo-chemical decomposition of organic matter at high temperatures in the absence of oxygen. When applied to biomass, it is a process complicated by the variety of the feedstock and of the pyrolysis conditions, which affect the production of a solid, a liquid and a gaseous fraction.[78] [79],[80] The yield of these fractions can be controlled by parameters such as rate of heating, temperature, pressure and the presence of additives. Typically, increasing the heating rate facilitates the production of volatiles.[81] The solid fraction (char) is endowed with a high carbon content; the liquid fraction (bio-oil) is a mixture of different organic compounds and water while the main components of the gaseous fraction are H_2, CO, CH_4.[82] The liquid fraction can be a valid alternative energy source for biofuels (for heat and power generation and transportation), while the pyrolysis gases are useful for heat or electricity production. [83] The solid fraction can not only be used as a solid fuel for the production of heat and electricity, but, due to its multifunctional properties, it can also be employed as amendment to improve microbial interaction in soils [84], biofertilizer [85], solid fuel [86], in effluent adsorption from palm oil milling [87], for catalytic applications [88].In addition, char will in turn be converted into activated carbon (AC) by using chemical or physical activation (see Paragraph 4.2). [89,90]. The process is usually performed by heating in electrical furnace or oven [91,92]. Alternatively, MW heating can provide a faster and more efficient pyrolysis process, since uniform heat is rapidly generated in a relatively short processing time when the biomass is irradiated by MW energy, allowing efficient pyrolysis decomposition to occur [93,94]. For these reasons, microwave assisted pyrolysis (MAP) has gained increasing interest in the last years to overcome the limits related to the non-selective electrical heating of conventional pyrolysis (such as heat transfer resistance and heat losses). Table 6 reports the comparison between MAP and conventional pyrolysis on waste biomass (CP):

Table 6. MAP versus CP

MAP	CP
Non-contact heating	Contact superficial heating
Lower energy consumption	Higher energy consumption
Rapid and uniform heating	Slow heating
Shorter reaction times	Longer reaction times
Improved product yields	Lower product yields
Broad range of feedstock, even large-sized	A reduced size of material is often required
Higher quality of products	Lower quality products
Reduced capital costs	High initial capital costs
Possibility to separate *in-situ* the products	Additional upgrading steps
Treatment of non-homogeneous waste, with no need for grinding	Biomass pre-treatment required

The higher heating rate (up to 42%)[95] of MAP compared to CP leads to less time and input energy involved in reaching the required temperatures. Therefore, even if high capital and equipment costs are required both in MAP and in CP, these are well compensated[96] by the process time savings and the enhanced yields of products achieved under microwaves. In addition, additional upgrading steps are necessary to separate the aqueous from the organic fraction and to improve the degree of functionalization of the products obtained under conventional conditions, thus implying additional separation costs. On the other hand, new chemical

profiles of the volatiles are described under MAP, thus enabling an in-situ upgrading of pyrolysis vapours.[1] Concerning the liquid fraction, MAP would make lignocellulosic biomass components produce more bio-oil than electrical heating pyrolysis, [97,98,99,100] and of higher quality. [101] Indeed, the chemical and physical properties of the bio-oil produced from MAP are much more similar to crude oil compared to the products obtained after conventional pyrolysis. In particular, the lower water content and the similar lower heating value (related to calorific value) makes the bio-oil produced via MAP a valid alternative to fossil fuels. [102] Also the solid fraction is of higher quality, showing higher calorific values and specific surface areas compared to the products of CP. MAP is advantageous not only for the quality of the products, but also because large-sized feedstock can be processed, as the heat exchanged from the external surface is lower than the heat produced by dielectric loss. Conversely, additional pre-treatment steps, including a size reduction of the starting material, are mandatory for CP, to enhance the thermal conductivity. Therefore, a huge reduction in the electricity consumption dedicated to the grinding and shredding processes can be achieved under microwaves. Therefore, also solid raw biomass with high moisture content, such as forest and agricultural residues, municipal solid waste (MSW) and sludge, can be efficiently treated using this technology, as a valid alternative to waste landfill disposal. Although MAP presents many advantages compared to CP, there are some limits. For example, in case of waste biomass possessing poor dielectric properties, the addition of MW absorbers becomes a prerequisite for pyrolysis. [103,104] Besides, the general applicability of the technology is still a challenge, as the optimization of the process parameters involving MW-heating is often feedstock-dependent. Even the same species grown in different locations and under different locations can show different behaviours under MAP.[105] So far, the most important parameters to optimize in MAP are the type, the size and water content of the raw biomass, the reaction temperature, the residence time, as well as the heating rate and the microwave power. [106,107] In particular, concerning this last parameter, several studies demonstrated an increase in gas yield but a decrease in solid yields with increase in MW power levels [318,351–358]. [108,109,110,111] However, the liquid production remained the same, while the kinetic parameters of rice straw pyrolysis increased. [112] The microwave type (multimode or single-mode) and the stirring may also influence the yield of products. [113] For example, Abubakar et al. [341] reported the effect of stirrer speed on the products of the pyrolysis of oil palm shell. [114] A decrease in bio-oil yield but an increase in gas yield was observed under enhanced stirring, which, at the same time, caused a decrease in the calorific value of char. Huang et al. underlined also the importance of the type and ratio of microwave absorbers and the location of the reaction flask inside the microwave reactor. [115,116] Concerning the type of feedstock, Ravikumar et al. studied the production of bio-oil by MAP of corn cob, corn stover, saw dust and rice straw. [117] By using a domestic MW oven (0.800 kW) for 10 min. at 400-500 °C, 15.3-42.1 wt.% yields were obtained depending on the feedstock used, with the least amount produced by rice straw, the highest from corn cob. The main products were oxygenated compounds such as carboxylic acids and phenols. Several waste biomass was employed as substrates for MAP: corn stover,[118,119,120,121] rice husk, sawdust and bagasse residues,[122] rice straw,[123,124] switchgrass,[125,126] Arundo donax.[127] Zhou et al. studied the effects of temperature and residence time in the pyrolysis of prairie cordgrass, using response surface methodology.[128] A temperature of 650 °C and a residence time of 18 min. afforded the maximum bio-oil yield (33.1%). Both aliphatic and aromatic compounds were found in the bio-oil, with a carbon size ranging from C4 to C20. Heating rate was proved as a significant parameter when comparing the MAP and the CP of moso bamboo.[129] The activation energy of the former is much lower, owing to the volumetric heating typical of microwaves.

4.1.1 Catalytic pyrolysis

As reported in the previous paragraph, the success of MAP depends on the dielectric properties of the material used as substrate. For this reason, MW absorbers may be added to the feedstock to promote the heating performance and initiate the pyrolysis process,[130] thus improving the efficiency of the process. Localized microplasma spots may occur in the surface of the absorbers, provoking a rapid increase of temperatures to very high values, thus leading to more energy efficient pyrolysis conditions. In addition, the product selectivity can be dramatically influenced by the addition of the proper catalyst. Typical pyrolysis additives are carbon materials or metal, metal oxides or hydroxides. Therefore, the type and the amount of

MW-absorbers and catalysts used play a crucial role in the product yields and quality. [131] The effects of the different conditions on the yields of the liquid, solid and gaseous fractions are summarized in Table 7. The bio char itself, produced during MAP, behaves as a MW-absorber due to its carbonaceous nature.[132] Typically, the presence of activated carbon prompts a decrease in bio-oil yield. This result can be explained by considering the elevated temperatures following the formation of hot spots on the carbonaceous material, which favour the cracking of biomass and bio-oil, with a decrease in bio-oil yield.[133] Besides enhancing the heating rates in the microwave field, chars and activated carbons can also show a catalytic effect in inducing a certain selectivity to target products. Indeed, it is worth noticing that activated carbon could considerably enhance the production of phenolic compounds in the bio-oil. For example, a phenolic-rich bio-oil (61.2% total phenolic content) was produced after the MAP of peanut shells and pine sawdust when activated carbon and was used as catalysts.[134] The MAP of switch grass was performed for 7 min. under a reactive gas atmosphere, using charcoal as an absorber, in order to investigate the influence of different gases in the pyrolysis products. [135] More deoxygenated products were obtained by using H_2, CH_4, and a model pyrolysis gas mixture, while CO decreased the bio-oil quantity and quality.

In principle, the heated material can either be used to obtain a valuable product or can be employed as a conductive source of heat transfer in several processes. In this frame, very recently Song *et al.* proposed the engineering of biomass derivatives with nitrogen doping for tailoring the dielectric and electromagnetic properties of the obtained carbon monolith [*136*].

A very novel study [137] reports on the combined use of MW and conventional heating by sequential application of MW for 30 min at 500 W and conventional heating to prepare AC from sunflower seed husk as raw material. $ZnCl_2$ (1:1 impregnation ratio) was added during activation for 45 min at 500 °C and materials with maximum BET surface area and total pore volume of 1511 m^2/g and 0.35 cm^3/g, respectively. On the contrary, other papers evaluated the potential of MW heating by comparing materials produced starting from the same feedstock but obtained by MW-assisted treatment and by conventional heating [138,139,140]. Suriapparao et al. investigated the effects of char and other absorbers (graphite, aluminum, silicon carbide, and an industry waste such as fly ash) for the MAP of *Prosopis juliflora*, a highly invasive lignocellulosic biomass traditionally harvested for combustion.[141] At 560 W MW power, with a biomass to absorber ratio of 100:1, the different absorbers afforded average heating rates in the order: SiC (70.86 °C min^{-1}) > char (64.27 °C min^{-1}) > aluminum (60.53 °C min^{-1}) > fly ash (52.56 °C min^{-1}) > graphite (30.32 °C min^{-1}). This trend is directly related to the gas yields. Concerning bio-oil, aluminium and fly ash led to the highest bio-oil yields (40%), instead, with the highest heating value achieved with SiC (29 MJ kg^{-1}), followed by aluminum, fly ash, char, and graphite. The different absorbers affected also the bio-oil composition. For example, high selectivity in linear ketones, acids and alcohols was obtained using fly ash, followed by aluminium and char. SiC was also used for the flash MAP of corn stover and wood sawdust, affording a maximum bio-oil yield of 64 wt% and 65 wt%, respectively.[142]

The microwave absorption can be further promoted by supporting metals on char. For example, Zhang et al. investigated the MAP of rice husk with rice husk char and rice husk char-supported metallic (Ni, Fe and Cu) catalysts.[143] The highest gas yield (53.9%) with a higher molar ratio of syngas (H_2/CO) was achieved using rice husk char-supported Ni catalyst. On the other hand, biochar-supported Ni and Fe catalysts enabled the tar removal. Ferrum-modified activated carbons play also a pivotal role in the composition of bio-oil. Indeed, when used in the MAP of Douglas fir, these catalysts prompt the increase of ketones (37.85% of bio-oil at 450°C and 8.00 min.), related to a significant decrease in guaiacols (18% of bio-oil). Even the phenols content was enhanced to 12 % after catalytic pyrolysis.[144] A part to organic materials, even soluble inorganics can be used as both microwave absorbers and catalysts to obtain more desirable products. The presence of inorganics, especially Ca and K, enables the decomposition of biomass and the generation of bio-char, [145] thus increasing the yields of the solid products. Catalysts such as K_2CO3 and NaOH (strongly polar) can dramatically absorb microwaves, determining extremely high temperatures inside the biomass, with the consequent enhancement in the gaseous products, becoming the predominant fraction. In particular, the activation energy during MAP is much lower when K_2CO_3 is used as the catalyst, underlining the importance of catalytic effect of the salt. For example, when the effect of different additives was compared (SiC, activated carbon, coke, K_2CO_3, and NaOH) on the product yields and characteristics after the MAP of sawdust,[146] it was observed that both K_2CO_3 and NaOH favoured the formation of gaseous products. Moreover, K_2CO_3 could simplify the bio-oil compositions, thus reducing the need for further separation.

The element of K is capable to catalyse the gasification reaction by the cracking of high molecular weight compounds under MW irradiation, affording small gaseous molecules (mainly CO and H_2). However, a higher bio-char yield was observed using K_3PO_4 as the catalyst, probably owing to the inhibition of devolatilisation of cellulose and hemicellulose, cause of an increase in bio-char production.[147] Even metal oxides are commonly used as MAP additives,[148] leading to an increase of the maximum temperature and the mass reduction ratio. In general, metal oxides possess redox characteristics owing to their multivalent nature and/or the acidic properties. These characteristics make them suitable catalysts for the thermal degradation of biomass and intermediates to more stable products. Many metal oxides, such as CaO, MgO, NiO, CuO, TiO_2, and Fe_3O_4, have been investigated as the catalysts for the catalytic MAP of biomass. For example, Huang et al. described the MAP of corn stover, one of the most abundant agricultural residue worldwide distributed. [149] At a power level of 500W, most of the metal oxide catalysts (NiO, CuO, CaO, and MgO) afforded solids with a lower calorific value and increased the production of liquids (probably owing to the Fischer–Tropsch synthesis). In addition, the formation of PAHs was strongly reduced, with a consequent reduction in the toxicity of the liquid products. On the other hand, the gas products yield was lower. The effects of metal oxides on the MAP of sugarcane bagasse were also investigated.[150] Herein, the authors observed a higher calorific value of the solid residues obtained after catalyst free MAP without any catalyst (24.38 MJ/kg) compared to the raw biomass (17.98 MJ/kg). The addition of the catalysts slightly lowered this value (22.84–23.94 MJ/kg), however, they keep them in a range already suitable for the application of the solids as biofuels. In addition, by the comparison of the different oxides, they reported that while NiO and CuO afforded higher liquid products yield, CaO and MgO enhanced the gaseous production. More in detail, during the comparable MAP system, the addition of CaO prompted a slight increase in the amount of H_2, while MgO showed the opposite effect. Contrary to the above reported, when NiO is coupled to Ni_2O_3, higher gas production rates and content of combustible gas were achieved.[151] In particular, with respect to catalyst-free conditions, NiO and Ni_2O_3 prompted the formation of CO and H_2 therefore lowering the CH_4 and CO_2 yields, as these catalysts promote not only the cracking of the organic compounds but also the CO_2 reforming reactions.[152]

The selectivity towards high desirable products, mainly in the liquid fraction, is one of the main issues occurring during biomass pyrolysis.[153] At the moment two types of bio-oils are mostly required: the hydrocarbon-rich bio-oil and the phenols-rich one. Generally speaking, the former can be obtained from the pyrolysis of a lignocellulose source, while the second comes from a predominantly lignin feedstock.[154] Despite this, an upgrading (i.e. further treatment with chemicals at certain temperature and pressure values) of bio-oil is usually required in order to obtain the desired products. [155] The use of zeolite-type catalysts, may help to reduce the need for the upgrading, as they strongly influence the selectivity of MAP, owing to their acidic properties and shape selectivity.[156] For example, ZSM-5 and modified ZSM-5 catalyst are normally used to produce hydrocarbon-rich bio-oil, even if one of the most extensively investigated zeolite is the HZSM-5, because of its strong Brønsted acidity, that promotes deoxygenation reactions to hydrocarbons. [157]

In summary, given the possibility to obtain high amounts of high-quality bio-oil, bio-char, and biogas by the proper choose of catalyst and additives, the catalytic MAP paves the way for an economically feasible valorisation of biomass on a large scale. [158]

Table 7: effect of the conditions of the catalytic MAP on the yields of the solid, liquid and gaseous fractions

Biomass	Microwave power	Temperature	Time	Catalyst	Gas yield (wt%)	Oil yield (wt%)	Solid yield (wt%)	Reference
Prosopis juliflora	560W	600 °C	15 min.	graphite	39.79	31.25	28.96	54
				char	42.45	32.95	24.60	
				aluminium	37.33	36.83	25.84	
				SiC	47.96	26.37	25.67	
				Fly ash	35.06	39.87	25.07	
Sawdust	750W	550 °C	12 min.	SiC	33	8	59	52
				coke	48	18	34	
				Activated carbon	48	28	24	
				K_2CO_3	59	23	18	

				NaOH	64	20	16	
Peanut shell	2000W	300 °C	50 min.	Activated carbon	32	11	57	53
Pine sawdust	2000W	300 °C	50 min.	Activated carbon	23	16	61	
Corn stover	750W	480 °C	2g/min* feeding	SiC	14	64	22	55
Wood sawdust	750W	500 °C	2g/min feeding	SiC	16	65	19	
Rice husk	700W	600	20 min.	RHC	46	16	38	56
	700W	710	20 min.	Ni/RHC	54	10	36	
	700W	750	20 min.	Fe/RHC	48	18	34	
	700W	680	20 min.	Cu/RHC	49	13	38	
Douglas fir	700W	450	8 min.	Fe on AC	36	37	21 [a]	57
Switchgrass	750W	400	2.8 min.	K_3PO_4	26	31	43	59
Corn stover	500W	520	30 min.	NiO	17	24	59	60
		500		CuO	16	22	62	
		510		CaO	15	28	57	
		480		MgO	16	32	52	
Sunflower seed husk	500W	500	30 min.	$ZnCl_2$	n.r.[b]	n.r.	n.r	64
Cellulose	700W	480°C	10 min.	ZSM-5	49	35	16	68

*Semi-continuous system, [a]Coke on catalyst (6%) was also observed. [b]Yields not reported

4.1.2 Low-temperature pyrolysis

The microwave-assisted processes described so far were all conducted at temperature similar to conventional pyrolysis (450÷600 °C), with the main scope of producing fuels. However, as already stated, the interaction of microwaves with the components of biomass can promote pyrolytic mechanisms at lower temperatures (<200°C), other than those occurring with conventional heating. Indeed, as the biomass components begin to decompose at temperatures 50-100 °C lower, the fastest weight losses occur at lower temperatures as well.[159] The weight loss behaviour of biomass components is related to the increase of the dielectric properties (due to the change in the structure disruption of the polymers) during the MAP process, leading to a thermal gradient and "hot spots" within biomass.[160] These phenomena are responsible for the acceleration of low temperature pyrolytic events. Therefore, a smaller number of compounds, different from the conventional ones, are detected in the bio-oil, making it a viable source of chemicals for the industry, according to a biorefinery approach. Besides changing the bio-oil composition, the low temperature MAP (LTMAP) can also decrease the yields of gas (from 43% under conventional pyrolysis to 25% under MAP at 180°C). However, the gaseous fraction contains higher amounts of syngas ($CO+H_2$), suitable for the synthesis of intermediates.[161] In addition, the composition of the bio-oil obtained at low temperatures is very similar to crude oil and depends on the starting biomass. For example, the bio-oil (21%) obtained after LTMAP of wheat straw in the 100-200°C temperature range contained less furfural and acetic acid compared to the conventional pyrolysis oil, and higher amounts of phenolic compounds.[162] Moreover, significant yields of long chain fatty acids (even hexadecanoic acid) were obtained. Interestingly, high amounts of levoglucosan and vinyl guaiacol are produced under LTMAP conditions. These are valuable chemical intermediates not present in the conventional pyrolysis oil. MAP is an important tool to overcome the problems related to the separation of the products. Indeed, it enables the *in-situ* fractionation of bio-oil into two fractions solely (the first containing water, aldehydes and acids, the second only valuable organics), based on the difference in their boiling points. In addition to bio-oil, 14% gas, 30% char and a further 35% of an aqueous fraction (containing 10% of low molecular weight acids and aldehydes) were obtained in these conditions. The char

is suitable for combustion as it was endowed with a good calorific value (27.2 kJ/g). Noteworthy, LTMAP enabled a total recovery of usable carbon of 70%, while conventional pyrolysis led to consistent carbon losses as CO_2 and CO.

LTMAP of rape meal well demonstrated the interaction of microwave irradiation with biomass at low temperature, resulting in sequential conversions of the different components.[163] At 100°C, virgin rape seed oil and residual water are removed via microwave steam distillation, thereby avoiding an additional hexane extraction step. Then, the biomass pyrolysis occurs in the 100-250°C temperature range, affording bio-oil, non-condensable gases, (chemisorbed) water and char. As in the previous case, the calorific value of the solid fraction was significantly higher compared to that of conventional char, making it a potential valuable fuel. This can be due to the higher hydrogen content of the char. In addition, the maximum calorific values were obtained at lower temperatures.

4.2 Hydrothermal conversion

As pyrolysis, hydrothermal liquefaction (HTL) is a thermo-chemical conversion technology, but, different from pyrolysis, it requires lower temperatures and, thereby, lower energy input. In addition, when applied to waste biomass, HTL affords mostly an aqueous fraction, with an oil fraction (bio-crude) which can be used a biofuel, and only small amounts of solid, aqueous and gaseous fractions.[164] However, very few works report the HTL for the production of bio-oil, the most of them referring to the conversion of algae, thus will be not taken into consideration in this paper. Conversely, HTL has been widely applied for the conversion of lignocellulosic biomass into valuable platform chemicals, as described in the previous section (3.1). Aiming at the biofuel production, hydrothermal carbonization (HTC) has been much more investigated, as an alternative to pyrolysis. This process takes place in an a inert environment and at a temperature range of 180-260°C, leading to the formation of mainly char (namely hydrochar) with small amounts of liquid and gas.[165] The solid fuel thus formed is endowed with a high carbon content and a high energy density, retaining 55-90% mass of the original biomass feed.[166]

HTC may be carried out either under conventional or MW-heating, given the inherent advantages provided by MW over the former. Indeed, MW-assisted hydrothermal processing is greener, faster and more efficient than the conventional one.[167] Moisture-rich biomass, such as shrimp wastes, that are normally recycled by uneconomical and not environmentally friendly methods, can be converted into hydrochar by hydrothermal carbonization (HTC), that is usually employed to treat lignocellulosic biowaste [168][169]. Agricultural waste, such as rice husk has a global annual production of 140 million tonnes and it is usually burnt in the fields or simply discarded, being both procedures detrimental from an environmental point of view [170]. Nizamuddin *et al.* investigated the effect of temperature, reaction time, biomass to water ratio, and biomass particle size on the hydrochar yield produced from MHTC of rice husks. Hydrochar with high heating value (16.10 MJ/kg) and increased surface area (92.69 m^2/g) was produced in 5 min at 1000 W and 220 °C with a yield of 62.8 %. The hydrochar carbon content was increased after MHTC, whereas both hydrogen and oxygen contents decreased, resulting in lower O/C and H/C atomic ratios. Other biomass wastes including rapeseed husk [171] as well as *Prosopis africana* shell [172]. The latter study reported a comparison of the chemical and structural properties of the hydrochars prepared starting from *Prosopis africana* shell (a waste plant) by MW-assisted (5–20 min) and conventional (120–240 min) hydrothermal carbonizations at 200 °C. Besides the shorter time of the MW process, the hydrochar produced under 20 min MW irradiation (M-$PAS_{200\text{-}20}$) shows similar decomposition to the same material produced by conventional heating (C-$PAS_{200\text{-}240}$). Scanning Electron Microscopy (SEM) images of the raw biomass and of the produced hydrochars (Fig. 14, sections A-C) put in evidence the morphologic transformation to which the *Prosopis africana* shells underwent upon HTC. Particularly the feedstock biomass displayed a cellular structure typical of lignocellulosic materials, whereas the two produced hydrochars are in the form of spherical particle agglomerates. The microparticles have size ranging from 1 to 10 μm, are formed during cellulose decomposition, precipitation and growth into spheres. On the contrary, lignin is only partially degraded because of higher thermal stability, originating the rough texture.

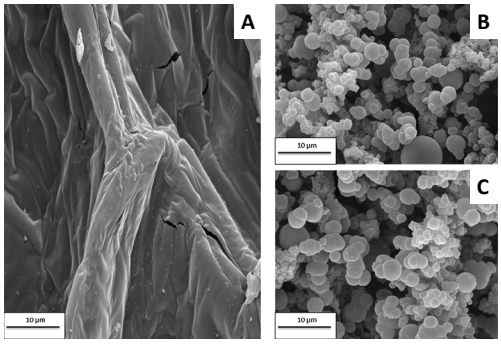

Fig. 14 SEM images of (A) raw *Prosopis africana* shell, (B) M-$PAS_{200\text{-}20}$, and (C) C-$PAS_{200\text{-}240}$. Reprinted from J. Anal. Appl. Pyrolysis, 118, E. S. Elaigwu, G. M. Greenway, Microwave-assisted and conventional hydrothermal carbonization of lignocellulosic waste material: Comparison of the chemical and structural properties of the hydrochars, Copyright (2016), with permission from Elsevier

5. **Microwave-assisted processes for biomass conversion into materials**

Due to moisture and volatile matter removal during the thermal treatment, the produced char possesses advantageous properties, such as porous structure, and surface functional groups along with mineral components, that lead to high reactivity of the material [173]. Despite these interesting features, biochar has restricted applications due to its limited functionalities [174], and it has poor porosity when not submitted to opportune activation, resulting in low adsorption capability of contaminants in polluted water [175]. However, if compared with traditional activated carbon, the feedstock to produce biochar are abundant and low-cost, since derived from agricultural biomass and solid waste [176]. As a matter of fact, biochar has an average price of \$ 2.65 kg^{-1}, ranging from of \$ 0.09 kg^{-1} to of \$ 8.85 kg^{-1}depending on the production sites (Philippines and UK, respectively) [177]. Therefore, biochar is a renewable and low-cost precursor for the AC production, thus, in the last years, the research has been focused on physical and chemical activation of biochar to improve its textural properties. [178,179,180,181]

5.1 On the activation of biomass residues

As stated before, It is necessary to submit the biomass waste (or the char obtained from it) either to physical or to chemical activation in order to improve the porosity of the material [182]. It has to be considered that biomass is not a homogeneous material, since it possesses non-regular shape, wide particle size distribution, high moisture content and low density. Moreover, along with different chemical compositions, biomass has different structures [183]. It was shown that the organs, such as rhizomes, stems rather than leaves play a key role on both yields and products coming from the MW-assisted pyrolysis of *Arundo donax* (a perennial cane all over the Mediterranean area) [184]. Depending on the adopted conditions, it would be therefore possible to emphasize or reduce such results.

Pre-treatment of biomass is considered one of the most expensive steps in the overall processing in a biomass-to-biofuel program. With the strong advancement in developing lignocellulose biomass and algal biomass-based biorefineries, global focus has been on developing activation methods and technologies that are technically and economically feasible. More in detail, carbon dioxide or steam are employed as activating agents in physical activation, whereas alkali metal hydroxides and carbonates are used in chemical one. The latter method has some disadvantages with respect to the former one, because it requires lower activation temperature, usually in the 450–700 °C temperature range, and activated carbon is produced with higher yield. Microwave pyrolysis can be coupled with chemical activation to produce AC [185]. However, it has been shown that chemical activation with phosphoric acid improves the biochar thermal stability, mesoporous structure [186], and surface acidity by means of oxygen–phosphorus surface groups formation [187,188]. Biochar chemical activation by H_3PO_4 presents some advantages with respect to the activation with H_2SO_4, firstly the

impregnation is carried out at ambient temperature rather than 150 °C, as in the case of sulfonation. In addition, biochar activation and carbonization are performed in one-step versus two-step carbonization and sulfonation. Finally, environmental issues have to be considered, since H_3PO_4 use results in moderate pollution by comparison with H_2SO_4 [189]. With the aim to clarify the effect the H_3PO_4 activating agent on the dynamics of MW heating (at 650 W) and on pyrolysis time, Villota *et al.* discovered that the pyrolysis got slower, when high amounts of activating agent are used, because H_3PO_4 favours poor MW absorption [190]. Moreover, phosphoric acid is converted into P_2O_5, requiring high activation energy, and further extending the pyrolysis time. Numerical optimization showed that AC with surface area of 1726.5 m^2/g can be obtained but will demand 84.83% H_3PO_4 for activation and 803.75 W MW power for 48 min for pyrolisis.

It has been reported very recently that MW-assisted pyrolysis of bagasse favoured the formation of electron-rich defective C/O atoms located at the edges of a graphite layer [191]. Such defects promote eventual further N/O doping by HNO_3 and H_3PO_4 addition, resulting in the presence of more N- and O- surface functional groups and in an increase of 3.5 times of the Cu(II) adsorption capacity of the material with respect to that produced by conventional heating.

Among the activating agents, potassium hydroxide was successfully used to obtain superactivated carbon from hydrochar [192]. Moreover, the use of a chemical mixture was reported to have beneficial effect on AC in terms of increased surface area and porosity [193].Very recently, plentiful literature extensively reviewed the effect of the activation parameters, such as temperature, time, gas flow rate, impregnation chemical, biochar ratio, on the final porosity formation in AC coming from lignocellulosic precursors [194], wood biomass [195], oil palm wastes [196], agricultural waste [197], and other sources [198] under MW irradiation.

A large variety of biomass precursors obtained from agricultural wastes (fruit shells, stones, husks, and hulls) and wood residues (chips and pellets) has been employed to obtain activated biochar [199]. It was found that: (i) high activation temperature [200, 201, 202, 203], as well as (ii) high flow rate of steam or CO_2 [204, 205], (iii) longer residence time (> 2 h) [206, 207, 208], and (iv) large impregnation ratio (amount of biomass: amount of activating agent) [209, 210, 211] contribute to the production of materials with high porosity. Moreover, it was reported that is possible to modify the biochar surface functional groups (carbonyl and basic groups) by regulating the temperature and residence time during the MW-assisted pyrolysis of corn stover at atmospheric pressure and at 600◦C [212]. The development of carbon surface functional groups, along with the optimisation of bio-oil, syngas and biochar production were described by a prediction model corroborated by FTIR spectroscopy. The amount of basic groups decreased with the increase of the temperature, possibly because of reduction in pyrone ligands during MW pyrolysis. As for carbonyl groups (0.27-1.70 mmol/g carbon), the change of its amount was more complex, because of biomass decomposition and vapour reforming. In **Figure 15** a representation of the response surface and of contour line modelled for the carbonyl groups amount is shown. At temperature > 600◦C, the amount of such groups increased by increasing the temperature and was diminished with the residence time, due to the occurrence of both dehydrogenation and demethanation. This lead to a big quantity of aromatic and to some oxygen functional groups. Conversely, at temperature < 600◦C, the amount increased with the temperature and residence time, because dehydration, decarboxylation and decarbonylation are mainly taking place at the biomass surface. Here, reactive free-radical sites are formed by decomposition of the surface oxides to CO_2 and CO [213].

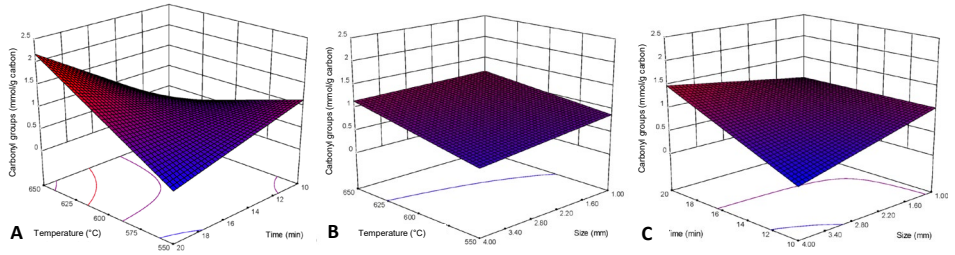

Fig. 15. Response surface and contour line of carbonyl groups amount as a function of reaction time (X_1, min), temperature (X_2, °C) and particle size (X_3, mm): (A) X_1X_2, (B) X_1X_3, (C) X_2X_3. Adapted from Journal of Analytical and Applied Pyrolysis, 115, L. Zhu, H. Lei, L. Wang, G. Yadavalli, X. Zhang, Y. Wei, Y. Liu, D. Yan, S. Chen, B.

Ahring, Biochar of corn stover: Microwave-assisted pyrolysis condition induced changes in surface functional groups and characteristics, 149–156, Copyright (2015), with permission from Elsevier.

Interestingly, the biomass particle size did not affect significantly the biochar surface functionality.
In a very recent paper, Liew *et al.* [214] proposed an innovative two-steps approach in which MW pyrolysis was combined with chemical activation by NaOH/KOH mixture to obtain a micro-mesoporous AC with surface area higher than that obtained when employing the one-step approach, in which carbonization and activation are simultaneously carried out. Indeed, during the first carbonization step, the largest fraction of banana peel volatile matter can be removed giving rise to pore formation within the non- volatile components that will originate the biochar. Subsequently, during the second chemical activation step, more pores will be formed along with the increase of width of the already existing ones, resulting in the production of the AC with improved surface area and porosity. In **Figure 16** the set-up of the microwave pyrolysis system is shown. As for the pyrolysis step, 1 L quartz reactor was used in combination with a microwave oven (frequency = 2.45 GHz, Samsung).

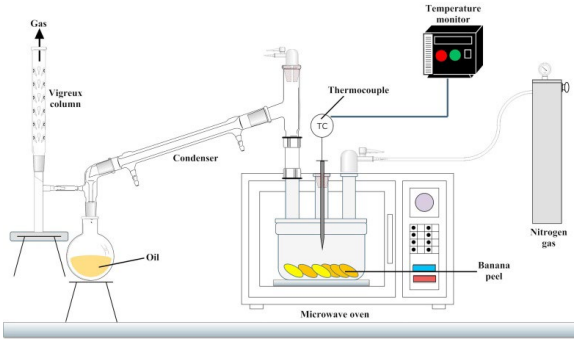

Fig. 16. Microwave pyrolysis system. Reprinted from Bioresource Technology, 266, R. K. Liew, E. Azwar, P. N. Y. Yek, X. Y. Lim, C. K. Cheng, J.-H. Ng, A. Jusoh, W. H. Lam, M. D. Ibrahim, N. L. Ma, S. S. Lam, Microwave pyrolysis with KOH/NaOH mixture activation: A new approach to produce micro-mesoporous activated carbon for textile dye adsorption, 1–10. Copyright (2018), with permission from Elsevier.

Banana peel is able to adsorb microwave and convert into heat energy, since its dielectric loss tangent is 0.375 [215] Biomass was submitted to for 20 min at 700 W of microwave power under a continuous N_2 flow of (0.25 L/min) at 800-900 °C, leading to 35 wt% char yields. To achieve chemical activation, 5 g of char was immerged for 24 h in a KOH + NaOH mixture solution with different chemical impregnation ratio (0.5, 1.0 and 1.5). The chemically activated biochar was then submitted to a second microwave pyrolysis at 400-500 °C to be converted into AC. The AC was produced with 29 wt% yield, low ash formation and < 5 wt% moisture. High BET surface area (≤ 1038 m^2/g) and micro-mesoporous texture with ≤ 0.80 cm^3/g pore volume were measured. Such features allowed up to 90 % adsorption of malachite green dye.
Magnetic biochars for agricultural waste biomass (*Triticum aestivum*) have been obtained very recently by combining MW heating with the addition of ferrofluid (an ammonia solution of precipitated Fe(II) and Fe (III) inorganic salts) to wheat straw in a one-step procedure [216]. These low-cost materials can be removed from the aqueous solution after sorption of As(V) species by simple magnetic separation. Another method to prepare magnetic absorbers using sugarcane bagasse feedstock by MW-assisted pyrolysis (power of 600 W) was reported by Mubarak *et al.* [217]. An optimum impregnation ratio (Fe_2O_3: biomass) of 0.45 was employed to obtain efficient absorbers for enhanced removal (96.17 %) of hazardous Cd^{2+} ions from aqueous solutions. Indeed, tiny microplasma spots within the biomass mixture during MW heating can favour the reaction at significantly low temperature, if compared to conventional heating [218,219]. Metallic Co and Fe subsceptors were reported to have beneficial effect in tailoring different biochar nanostructures, along with the in production of bio-oil and gases, by MW (600 W) pyrolysis at 500 °C of sugarcane bagasse at relatively low temperature and time [220]. In particular, nanoparticles and nanotubes and graphitic flakes were formed upon iron addition, whereas an increase in the Fe amount leaded to coalescence of such nanostructures, due to

an enhancement in localized heating. However, in addition to an enhancement of the net carbon content and crystallinity, Fe addition favoured high yield of gases and low yield biochar, without affecting bio-oil production. On the other hand, the Fe and Co co-addition resulted in the production of small graphitic flakes surrounded by fine nanotubes. Thus, microwave pyrolysis is shown to be a promising technique to tailor the morphological features of biochar by using metallic susceptors, and simultaneously produce good quality bio-oil and gases.

Pores with narrow sizes, along with carbons with high surface area are produced in the presence of $ZnCl_2$, that for this reason is considered an outstanding chemical activating agent [221,222]. Thue *et al.* investigated the effect of the addition of $CoCl_2$, $NiCl_2$ and $CuCl_2$ on the physicochemical properties of the ACs prepared by MW-assisted pyrolysis of a wood biomass (*Entandrophragma cylindricum or Sapelli*), that have been tested for the adsorption of organic pollutants from aqueous solutions [223]. FTIR and Diffuse Reflectance UV–vis spectroscopies revealed that the metals were linked to the biomass surface functional groups by ionic or covalent bound. The AC surface areas increased with the metal: biomass ratio, as well as the total pore volume. It was also observed that (i) the Co-based AC sample was able to adsorb more o-nitro phenol compared to traditional Zn-AC sample, (ii) Cu-AC, Co-AC and Ni-AC possessed hydrophobicity indexes > 1, resulting in hydrophobic AC materials, (iii) the samples displayed high values of carbon contents and oxygen-containing groups, and (iv) the adsorption capacity was: Zn-AC > $CuCl_2$ > $CoCl_2$ > $NiCl_2$, in agreement with atomic number and melting point trends (Ni(II) < Co(II) < Cu(II) < Zn(II)), instead of the Irving-Williams series.

5.2 Microwaves to prepare activated carbons

The biomass is converted into biochar by pyrolysis to obtain activated carbon. AC is a functional material, which is characterised by large specific surface area, superior porosity, high physicochemical-stability, and excellent surface reactivity, that is commonly employed for several applications [224], such as adsorbent for the removal of organic pollutants [225] and carbon dioxide sequestration [226]. AC has a global market size that in 2012 was USD 2 billion in 2012 and that is expected to be USD 4 billion in 2019 [227]. AC is traditionally produced starting from wood, coal, petroleum residues, peat, lignite and polymers, which are very expensive and non-renewable [228]. As a consequence, the use of low-cost and sustainable precursors, including agricultural wastes (as for example rice husk, corn straw and bagasse) and other solid wastes (as for example garden waste and sludge) to prepare AC [229] gained attention for the economic feasibility of large scale production. In this frame, F. Mechati *et al.* obtained different AC able to efficiently remove methylene blue from aqueous solutions [230]. Vegetable wastes were activated with H_2SO_4 and further pyrolysed in inert nitrogen atmosphere under MW (400 to 650 W) for 3-6 min. They chose either hard biomasses, such as apricot and peach stones, or soft ones, such as peel orange and grape stalk, and found interestingly that the hard precursors possess improved porous structure with respect to that of the soft bio-wastes. Indeed, AC obtained from apricot and peach stones have BET surface area of 529 and 518 m^2/g, total pore volume 0.26 and 0.25 cm^3/g as well as microporous volume of 0.19 and 0.20 cm^3/g, respectively.

Low cost AC was also obtained from post-agricultural waste (low quality hay) by MW pyrolysis at 700 °C for 60 min under nitrogen flow (0.170 L/min) [231]. The produced char was then submitted to physical MW activation either at 700 or at 800 °C under carbon dioxide flow (0.250 L/min) for 15 and 30 min. Despite low surface area and porosity, these ACs are potential efficient adsorbents for the abatement of acidic pollutants (NO_2, H_2S) due to their surface basicity.

Another common low-cost agricultural waste such as oil palm shell waste (> 4.7 million tonnes in Malaysia in 2007) was employed to prepare high area ACs MW heating and KOH activation under CO_2 (1195.6 m^2/g) or N_2 (1630.4 m^2/g) flow [232], due to the capability of the former activation agent to react and to generate more pores. On the contrary, the ACs obtained under N_2 flow display enhanced ultramicroporosity.

Starting from waste cumin and hydrochloric and hydrofluoric acids washed cumin plants, AC was produced by MW-assisted carbonisation in the presence of H_3PO_4 as the activating agent [233]. The washing step with HCl and HF removed the mineral matter contained in the waste biomass before activation. Then the raw cumin material along with the acid washed samples were treated with H_3PO_4 and further submitted to MW carbonisation. The AC electrodes showed improved performance due to the absence of mineral matter.

Olive stone biomass was activated by KOH addition and submitted to either MW-assisted or conventional heating [234]. AC with superior BET surface area along with excellent Ni^{2+} absorption capacity (>99.9 %) was

produced in higher yield (86.05 vs. 74.79 %) by MW heating (565 W) at 715 °C in a significantly shorter time (7 min vs. 2 h). Standard full factorial statistical design of experiments was employed to optimise the process: MW radiation power, radiation time, and impregnation ratio strongly influenced both yield (Fig. 17, sections A and B) and Ni^{2+} removal, making such materials suitable for commercial manufacture.

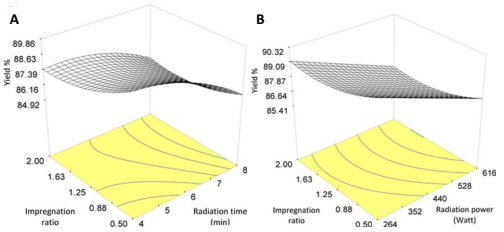

Fig. 17. Three-dimensional response surface plot: (A) MIOS yield (effect of radiation power and chemical impregnation ratio, *t* = 7 min), and (B) MIOS yield (effect of radiation time and chemical impregnation ratio, radiation power = 565 W). Adapted from T. M. Alslaibi, I. Abustan, M. Azmier Ahmad, A. Abu Foul, AIChE Journal, 60, 237-250, Copyrght (2014) John Wiley and Sons.

A similar approach, i.e. comparison with conventional heating and activation with KOH, was adopted by Jia *et al.* for the MW-assisted pyrolis (1200 W) of pulp mill sludge in a few minutes [235]. AC with BET specific surface area of 660 $m^2\ g^{-1}$ was obtained, and it was found that a 5 % mass fraction of KOH acted as a MW absorber and guaranteed full sludge conversion. Moreover, in the MW process, the retained carbon was 20 % lower than in conventional heating, because of the quicker volatile release under MW irradiation.
With the aim of efficiently removing waste residue of vineyards, MW pyrolysis of crops from *Vitis vinifera* was performed with a multimode MW oven in the presence of different MW absorbers (carbon, Fe powder, SiC) [236]. It was observed that by opportunely choosing the absorber and the reactor arrangement, it is possible to direct the product yield either to a high bio-oil (34.9 %) and gas (45.7%) production or to large amounts of bio-char (71.4 %). Very recently, biomass-derived ACs with three-dimensional porous architecture and large BET specific surface area (1229 m^2/g), were produced by MW-assisted carbonization combined with KOH activation of camellia oleifera shells [237]. The presence of electrochemical-active oxygen-containing surface functional groups improved significantly the supercapacitive performances.
In view of MW processes design optimisation at large scale, Binner *et al.* very recently shed light for the first time on the intermediate steps of MW-assisted pyrolysis (single-mode high field MW reactor) without adding any MW susceptor and performed a careful investigation on the effect of the operating parameters (input power, absorbed energy and processing time) on the functionality of the produced AC material starting from waste pecan nutshells (*Carya illinoinensis)* biomass [238]. The authors put in evidence that the intermediate products during MW pyrolysis are different from those of conventional pyrolysis due to biomass–MW interactions. Particularly, selective MW heating gives rise to the degradation of (hemi)cellulose and lignin processes at the same time, differently from conventional pyrolysis in which these processes occur sequentially. High energy MW inputs (> 4 kJ/g) produced more ordered char structure, consisting in plate-like graphitized aromatic sheets, with respect to that obtained by conventional heating up to 650◦C, corresponding to an increase of dielectric loss above 550 °C (F. 18, sections A and B). Moreover, the AC BET specific surface area firstly increase upon MW exposure, but at high adsorbed enery (6 kJ/g) and power a loss of specific surface area is observed (section C), due to the occurrence of overheating degradation and melting of the microporous structure, leaving resulting in a mesoporous material. However, it was demonstrated that BET surface area and porosity were not crucial in lead removal efficiency of these ACs. Indeed, the Ca components present on the MW-prepared materials are determinant for effective Pb removal of lead and correlate with MW energy input.

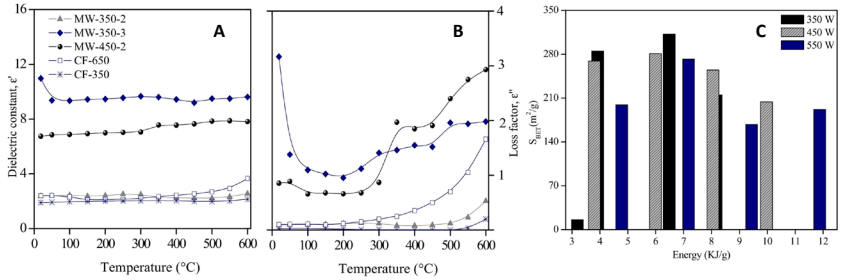

Fig. 18. Comparison between dielectric properties of carbon samples produced by microwave treatement at different conditions (MW-350-2, MW-350-3, MW-450-2), by conventional heating at 650 °C (CF-650) and 350 °C (CF-350) (A). Specific surface area (S_{BET}) as function of the energy absorbed during the treatment. Reprinted from Journal of Analytical and Applied Pyrolysis, 124, G. Duran Jimenez,T. Monti,J.J. Titman,V. Hernandez-Montoya,S.W. Kingman,E.R. Binner, New insights into microwave pyrolysis of biomass: Preparation of carbon-based products from pecan nutshells and their application in wastewater treatment, 113-121, Copyright (2017), with permission from Elsevier.

It has been reported that physical activation of charcoal produced starting from Kraft lignin by MW plasma favoured the development of enhanced porosity. The BET surface area (468 m^2/g) increased of 63 % with respect to the original surface area [239].

5.3 MW-assisted production of carbon nanotubes, LEDs, carbon dots and r-nGO,

MW-induced biomass gumwood pyrolysis carried at 500 °C favoured a vapour−solid phase growth process for producing multi-walled carbon nanotubes (CNTs) without adding any supplementary catalyst, substrate, or source gases [240]. However, SiC receptor was used to improve MW absorption by the employed biomass. The CNTs have a diameter of 50 nm along with a wall thickness of about 5 nm. The authors proposed a growth mechanism involving surface selective heating, able to create superheated active sites on which graphitized carbon self-assembly takes place forming CNTs (Fig. 19).

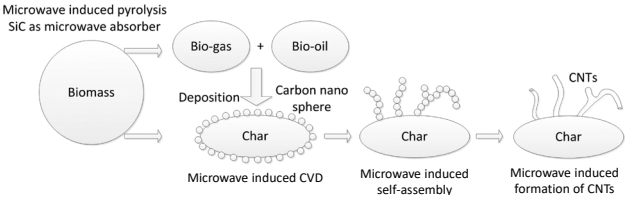

Fig. 19. Mechanism of the growth of CNTs via microwave-induced pyrolysis of biomass. Reprinted with permission from K. Shi, J. Yan, E. Lester, T. Wu, Catalyst-Free Synthesis of Multiwalled Carbon Nanotubes via Microwave-Induced Processing of Biomass, Ind. Eng. Chem. Res. 2014, 53, 15012−15019. Copyright (2014) American Chemical Society.

Particularly, volatiles released from the gumwood under MW irradiation left behind char particles (originating from biomass), which in turn behave as substrates. In this contest, the mineral matter present in the char particles catalysed the CNT growth, whereas the released volatiles served as carbon source gas. Then volatiles underwent thermal and/or catalytic cracking on the char surface, resulting in the formation of amorphous carbon nanospheres, which self-assembled to form multiwalled CNTs under MW irradiation.
In another very recent paper, green deep eutectic solvent (DES), i.e. oxalic acid and choline chloride, were employed to achieve ultrafast lignin removal from wood under MW irradiation [241]. The lignin was partially dissolved by DES (process I) as shown in Figure 20, section A. After MW-assisted heating in DES, the colour of the wood changed into dark brown, meaning that a high content of lignin was extracted. Then the residual lignin was removed by a treatment with an alkaline H_2O_2 bleaching solution (process II, section B) and the

colour became progressively white, due to the light reflection at the interfaces. Sections C and D illustrate the content change of lignin and cellulose. It is worth noting that > 90 wt % of lignin was removed, and the cellulose skeleton structure of the wood was maintained between wood cells.

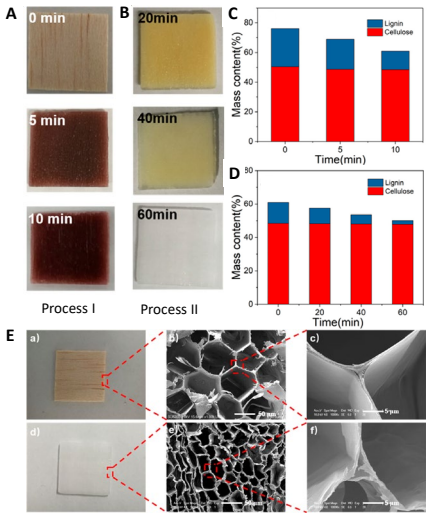

Fig. 20. Colour changes of wood during lignin removal process I (A) and II (B). Lignin and cellulose content of wood during lignin removal process I (C) and II (D). Photo images (E) of original wood (a) and lignin-removed wood (d). Cross-section SEM images of cell wall structures of original wood (b) and the lignin-rich middle lamella (c). SEM images of cell wall structures of the delignified wood chip (e) and the empty middle lamella (f). Adapted with permission from Z. Bi, T. Li, H. Su, Y. Ni, L. Yan, Transparent Wood Film Incorporating Carbon Dots as Encapsulating Material for White Light-Emitting Diodes, *ACS Sustainable Chem. Eng*. 2018, **6**, 9314−9323. Copyright (2018) American Chemical Society.

SEM images (section E) before (b) and after (e) DES delignification and bleaching did not show micro-damage, channels of 150−200 µm were observed. However, the rigid cell wall turns into flexible, revealing efficient lignin removal, and cell wall separation in the middle lamella occurred (f). Carbon dots and poly(acrylic acid) were then polymerized *in situ* to fill the obtained porous cellulose-based frame, resulting in a transparent wood film embedding multicolour carbon dots with enhanced mechanical tensile strength (60.92 MPa). The transparent wood can be employed as an alternative encapsulating material for white light emitting diodes.
Photoluminescent carbon dots (CDs) were synthesised by microwave-hydrothermal treatment of goose feathers [242]. Due to the heteroatom-rich composition of goose feathers, the produced CDs have uniform morphology and narrow size distribution (Fig. 21, sections A and B). These microstructures were ascribed to the b-keratin precursors (four repeating units of two b-sheets) and are characterised by a broad absorption with a shoulder at 270 nm (section C), due to the p–p* transition within the carbon framework.
The light yellow CDs suspension turned into strong blue luminescence upon excitation at 365 nm (section D). It is worth of note that such one-step simple synthesis process does not imply the use of strong acidic solvent or surface modification reagent, resulting in an effective process for large-scale production of photoluminescent CDs.

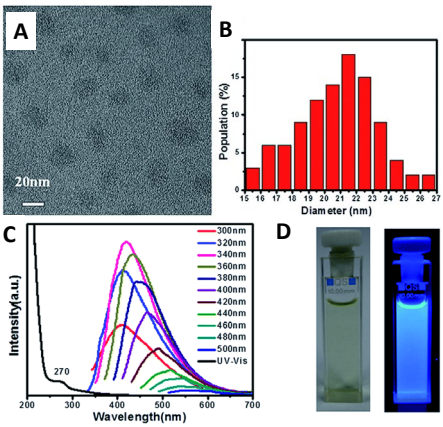

Fig. 21. (A) high-resolution TEM image of the CDs from goose feather; (B) CD size distribution histogram; (C) UV-Vis absorption and photoluminescence emission spectra (recorded for progressively longer wavelengths with 20 nm increments from 300 nm to 500 nm) of a dilute aqueous suspension of the CDs; (D) photographs of the suspension of the CDs taken under daylight (left) and excitation at 365 nm (right). Republished with permission of *RSC Adv.*, A facile microwave hydrothermal approach towards highly photoluminescent carbon dots from goose feathers, R. Liu, J. Zhang, M. Gao, Z. Li, J. Chen, D. Wu, P. Liu, 5, 4428-4433, 2015; permission conveyed through Copyright Clearance Center, Inc.

M. Hakkarainen *et al.* successfully reduced cellulose derived nanographene oxide (nGO) type carbon nanodots by hydrothermal treatment under MW irradiation (950 ± 50 W) in the presence of either superheated water or of a green reducing agent (caffeic acid, CA) [[243]]. Both biobased reduced nGO (r-nGO and r-nGO-CA) carbon nanodots possessed low oxygen content and an increased amount of sp^2 hybridized functional groups. Superheated water and CA were shown to have a synergistic positive influence, in terms of highest C/O ratio and thermal stability higher than that of nGO. These materials displayed excitation dependent fluorescence behaviour, in addition nGO and r-nGO-CA exhibited nontoxic behaviour to osteoblastic cells MG-63 up to 200 μg mL^{-1} and 1000 μg mL^{-1} respectively, giving rise to possible biomedical applications.

6 Scale-up and limiting issues in industrialization of MW-assisted process

When considering the possibility to scale-up the processes, energy efficiency is a fundamental parameter to be taken into consideration. Concerning MAP, not only the reduction in reaction time can contribute to increase the efficiency, but also the reduction in the downstream post-pyrolysis processes, such as the upgrading and separation of the products.[244] However, the scaling up of biomass pyrolysis is still at an early stage, as other issues should be considered.

First of all, the limited penetration depths of MW through the material, that conditions the size of the vessel and thus the actionable biomass. To overcome the main drawbacks related to microwaves, some studies investigated the move from batch to continuous systems. [245] Indeed, the continuous can accelerate process intensification. For example, Robinson et al. reported the design of a continuous processing system as a viable tool for the large-scale MAP of larch, to maximize the bio-oil quantity and quality. [246] In this case, a cold sweep gas is necessary to quench the pyrolysis products. To avoid gasification due to large-scale thermal runaway, the temperature must be kept under 500°C, thereby the use of microwave absorbers will not be feasible for pyrolysis of biomass on an industrial scale. It has been postulated that the use of new absorbing additives, obtained, for example, by doping nanoparticles on MW absorbers, may help to overcome this problem, by reducing the thermal runaway effect. [247]

In addition, to lead the MAP technique to an industrial level, a deep investigation into the key parameters that affect the process is necessary.[248] Considering the equipment, a pressure window is mandatory to

separate the waveguide from microwave cavity, in order to prevent the fouling of the handling system and the damage of magnetrons.[249]

Some studies analysed the scalability of MAP from an economic point of view. For example, Wang et al. described the catalytic mobile MW pyrolysis system, producing an aromatic hydrocarbon enriched bio-oil, gas and biochar. The authors demonstrated that with this set up, a high profit could be gained annually, with a return of investment of 45.34% per year, also coming from the increase in the bio-oil yield.[250]

As stated before, the production of biochar is of great interest since it can be converted into activated carbons for several applications. China is the worldwide leader in the production and exportation of all types AC, being the producer of about half to the total production and having exported 232.5 thousand tons in 2012. In August 2007 the U.S. disposed five years antidumping duty for AC importation from China, resulting in an import decrease to the U.S., and in importation mainly from India and neighbouring American countries. Due to more severe pollution controls and to an increasing consumer goods demand, the worldwide production of AC is increased by 58% in 2016 (1.9 million metric tons) and it is expected to grow up constantly at an annual rate of 10.3 % [251] and it is projected to overcome $4.9 billion by 2021 [252]. Moreover, government regulations dedicated to pollution control become ever stringent, making activated biochar an appealing alternative for the AC market.

As already explained in Section 4., AC can be produced starting from non-renewable coal by conventional heating in a furnace and by subsequent steam activation. This thermal process is energy and cost intensive, whilst the AC production using MW energy represents a promising alternative. Indeed, uniform heating and higher rates of heat transfer lower the energy consumption, shorten the time, and compact processing equipment, resulting in drastic decrease of the capex and opex of the plant. In addition to these issues, in these recent years many industries, operating in the agriculture, logging and forestry fields, convert biomass residues into biochar in order to handle the tons of waste generated every day. However, very few papers have been published on the pilot scale MW assisted production of AC [253,254,255].

Nevertheless, most of the studies on the MW-assisted production of AC have been performed by using a household microwave oven. Moreover, useful information on the scale-up of the equipment to industrial scale is not reported. However, the use of culinary microwave ovens, even if a quartz reactor inside the cavity, has important limitations: (i) it is difficult to find a quartz reactor with adequate shape and size; (ii) the quartz reactor limits the batch size; (iii) 800–1000 W is the maximum microwave power and (iv) the single standing electromagnetic wave would originate an inhomogeneous temperature distribution. The uniformity of temperature distribution has been recently investigated by simulations in the experimental equipment design [256]. Pianroj *et al.* [257] in order to work with increased biomass temperatures, designed a MW cavity equipped with two waveguides (operating in TE01 mode, with dimensions 8 cm, 10 cm, and 4 cm height) from two commercial MW magnetrons operating at 2450 MHz and they modelled and predicted the electromagnetic fields, having in mind that adding magnetrons to increase MW power, due to the interference of standing waves inside the cavity, represents a low-cost solution. Moreover, the combination of the two magnetrons ~~gave~~ markedly enhanced the pyrolysis temperature, given the same power (800 W) for 1–90 min time range. The bench-scale MW pyrolysis equipment was tested in the pyrolysis of oil palm shells. The MW pyrolysis system scheme is shown in detail in Figure 22, section A.

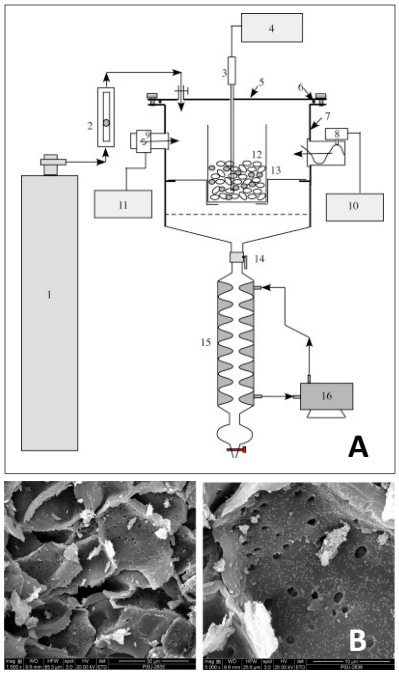

Fig. 22. (A) Schematic diagram of the microwave pyrolisis system: (1) nitrogen gas, (2) rotameter, (3) thermocouple, (4) temperature display and data logger, (5) microwave cavity lid, (6) rubber lid seal, (7) microwave cavity, (8) right magnetron, (9) left magnetron, (10) microwave power supply for right magnetron, (11) microwave power supply for left magnetron, (12) sample mixture of biomass and AC, (13) quartz reactor, (14) entrance valve, (15) condensing unit, and (16) cooling water pump. (B) Surface morphology of bio-char from microwave pyrolysis, with the SEM magnification 1500× (left), and 5000× (right). Adapted from Chem. Eng.Process., **106**, Y. Pianroj, S. Jumrat, W. Werapun, S. Karrila, C. Tongurai, Scaled-up reactor for microwave induced pyrolysis of oil palm shell, 42–49, Copyright (2016), with permission from Elsevier.

The one-liter commercial quartz reactor has cylindrical shape and the temperature was monitored by a type-K OMEGA grounded thermocouple to avoid arcing under microwave irradiation. In this case, active charcoal was added to the oil palm shells in different ratios (75:25, 50:50, and 25:75) in order to enhance the absorption of microwaves. The biochar was obtained by pyrolysis at 700 °C and its surface morphology was characterised by SEM, showing many pores without any crack (section B) and has heating value of 29,200 J/g. Many factors (MW penetration depth, employed materials to construct the reactor under MW irradiation, thermal insulation materials, manufacturing capability of MW components, types of biomass and their properties, reactor types, batch or continuous operations, and process related costs) have to be evaluated when scaling-up a MW-assisted process [258]. Depending on the different biomass feedstocks, the scale-up law for a particular reactor type (such as fixed beds, auger reactors and fluidized beds) has to be observed. Most important within the scale-up of the process are the peculiar features of MW heating as well as the associated costs [259]. Particularly, the depth of MW penetration is correlated to the MW frequency, but also to the temperature of the process and to the dielectric properties of the biomass. The higher is the MW frequency, the smaller is the MW penetration depth [260]. Generally, a magnetron with low MW power is not expensive, whereas the cost is increased when the capacity of the magnetron increases. Therefore, the most economical solution in industrial MW processes is to employ systems including multiple magnetrons. In this frame, either at lab scale or for demonstration plants, the most common materials used for MW reactors are materials with small dielectric loss factors (such as quartz, glass, porcelain, etc.). At the moment, the available

size of commercial tubes and vessels (0.5–1 m) limits the capacity. Moreover, a careful choice of the feedstock with appropriate compositions is strategic to produce AC with designed properties for specific applications. In this frame, the AC precursor properties have be carefully estimated and characterised, since the more MW energy the AC precursor is able to absorb, the higher is the MW energy amount that the material of the reactor captures, resulting in higher system efficiency [261].

To achieve high energy efficiency, the insulation materials with small dielectric loss factors play a key role, especially when the activation and/or carbonisation MW-assisted processes are carried out at high temperatures. Obviously, all these factors are strictly connected to each other and should be integrated to achieve a cost sustainable and reliable scale-up. Nevertheless, the application of the parameters obtained from small facilities is not feasible to large plants.

As already discussed, biochar applications are restricted by the low porosity and surface area (< 200 $m^2 g^{-1}$) induced in the material by the experimental conditions adopted in large-scale reactor [262]. For example, pyro-gasification is performed at 320 °C max, the residence time is limited to 1–2 s, and the heating rate is very high (1000 °C min^{-1}). A pilot-scale torrefaction/pyrolysis and activation plant was used to prepare activated biochars coming from different wood residues (black spruce and white birch) [263]. **Figure 23** (section A) reports a representative scheme of the torrefaction/fast pyrolysis plant (CarbonFX technology, Airex Energy Inc., Bécancour, QC, Canada) in which biomass, largely available in Abitibi-Témiscamingue, in the province of Québec, Canada, can be converted to biochar (or torrefied material) at temperature ranging between 250 and 455 °C in an anaerobic environment.

A cyclonic bed reactor was used to process the biomass allowing large-scale biochar production (up to 250 kg h^{-1}). This reactor is suitable to work with several feedstocks, such as woody biomass and agricultural waste, according to the following steps: (i) biomass drying (40-70 °C) in a pre-drying system, (ii) conditioning (480-650 °C, the biomass is transported into the conditioning chamber), (iii) combustion (480-650 °C, the biomass is transported from the conditioning chamber to the combustion chamber). Then, (iv) conversion into torrefied biomass or biochar in roughly 2 s inside the cyclonic bed reactor (300-480 °C). The system parameters (temperature process, percentage of oxygen inlet, hot air flow, and residence time in the cyclonic bed reactor) are controlled by a control panel. Before the introduction in the reactor, the wood wastes were milled and dried to achieve a moisture content < 40 %. Section B of **Figure 23** shows the 1 kg charge pilot furnace used to activate the waste. Such pilot-scale furnace was developed by the CTRI laboratory for biochar activation and is composed by (i) the hopper to feed the precursor material, (ii) the screw conveyor tube (the material took 67 min to pass through), that is located inside a muffle furnace, and (iii) the hopper for the recovery. Gases and organic compounds released during activation are condensed in the condensation tube, whereas nitrogen and to CO_2 are introduced by additional gas inlets. The authors found that the pyrolysis (315-450 °C) and activation temperatures (700-900 °C), as well as activation gas injection, particularly the CO_2 gas flow rate (at $p < 0.05$), and the type of wood residue strongly affected the resulting textural properties of the activated biochars, in terms of surface area, total pore volume, micropore volume, and amount of mesopores. A statistical model analysis allowed to control the porosity by varying the process parameters to obtain materials with specific porosity. With respect to small-scale furnaces, the sale-up of the activation furnace could in principle diminish the heating efficiency of and mass transfer in the char bed, hence lowering the porosity of materials. However, with such system activated biochars of 400-900 $m^2 g^{-1}$, comparable with similar biochars produced by using laboratory-scale furnaces, can be obtained.

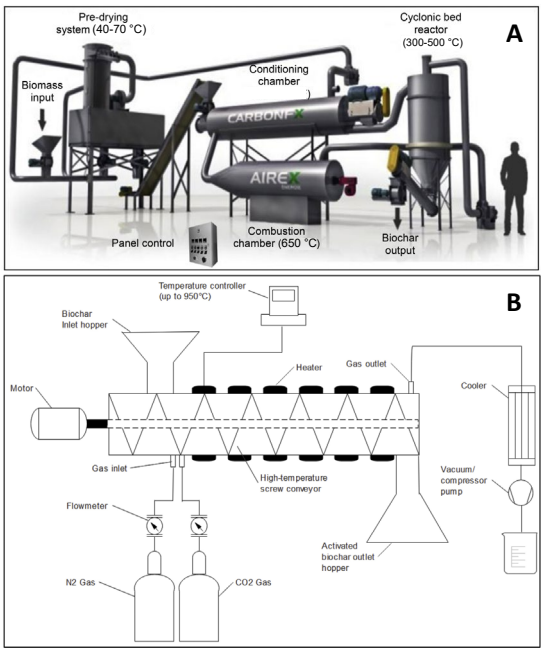

Fig. 23. (A) Pilot-scale fast pyrolysis unit (CarbonFX, Airex Energy); (B) Biochar activation furnace developed at CTRI (Center Technologique des Résidus Industriels –Technology Center for Industrial Waste), QC, Canada. Reprinted from *Biomass Bioenergy* **118**, F. L. Braghiroli, H. Bouafif, N. Hamza, B. Bouslimi, C. M. Neculit, A. Koubaa, The influence of pilot-scale pyro-gasification and activation conditions on porosity development in activated biochars, 105–114. Copyright (2018), with permission from Elsevier.

Hence, activated biochar with specific properties can be designed and produced to address to target applications, by strategic selection of the process parameters. A screening of the composition of different feedstock, the optimization of pyrolysis parameters, such as temperature, heating rate and residence time, and the choice of the physical, chemical or combined activation method, as well as the optimization of the activation parameters (nature of the activating agent, temperature, and time) allow to modulate porosity and surface chemistry of the desired material [264].

There are some limiting issues that have to be taken into serious consideration when scaling-up the reactor, in order to achieve high throughputs. Firstly, it is important to dry biomass to an optimal moisture content before introducing into a MW reactor, because the higher is the biomass moisture content, the higher is the corresponding dielectric loss factor [265], resulting in an increased efficiency of the process. On the contrary, high moisture amounts can favour vaporization, causing energy loss. Indeed, there are several recent research papers regarding the MW-assisted AC production which do not specify appropriately the information to characterize the biomass. For example, the moisture contents of biomass are not fully reported [266,267,268,269]. Another parameter that is often omitted is the biomass bulk density. Such information could be useful during the scale-up planning design to ascertain the compactness of the equipment. Moreover, it should be better to indicate the molarity of the activating agent solution and the g of activating agent/g biomass after drying.

The accurate measurement and control of biomass temperature inside the microwave reactor is a critical issue. Usually, a small amount quantity of activated carbon (with high loss tangent) is added to the biomass to improve the heating efficiency. The temperatures of both surface and bulk of the bed inside the MW reactor deviate when low amounts of MW absorption material are employed, whilst they converge when high amounts are added [270]. In this frame, the stirring speed has been reported to have beneficial effect on

the temperature uniformity within the bed. Therefore, to work with a system with uniform temperature, the amount of inert dielectric material with high loss tangent along with the stirring rate have to be carefully optimised. To estimate the heat generation rate and temperature profile inside the reactor, the dielectric properties have to be carefully evaluated when scaling-up the microwave reactor. Indeed, voltage breakdown and arching could occur at high external electric field stress and low pressures, damaging both process and product. Along with voltage breakdown, thermal runaway is the primary safety concern in the scale-up of a microwave reactor.

7 Preliminary life cycle assessment considerations

Industrial processes utilize almost 25 % of the energy consumed in Europe [271]. To diminish the energy required by industrial processes, MW represents a promising alternative solution. At the moment MW heating is usually employed in many low temperature industrial processes (such as drying) and low power demand. Nevertheless, at the moment, high temperature MW heating has not yet been optimised for full-scale industrial processes [272].

Life cycle assessment (LCA) aims at evaluating the environmental issues related to a specific product, process or activity. Energy, along with employed materials and produced wastes released to the environment are identified and quantified along with the possibility to improve the environmental sustainability [273,274,275,276]. The methodological approach for LCA studies is defined by the International Standard ISO 14040-4 and it is divided in four main steps: (i) definition of goal and scope, (ii) inventory analysis, (iii) impact assessment, (iv) interpretation.

Emissions would be displaced by introducing MW heating systems in industrial applications, because fossil fuel combustion to generate heat would be avoided. As a “full-electric” process, the MW heating system has definite carbon emission reduction potential. Indeed, the MW process allows an energy reduction in terms of process energy demand, considering that the MW electric feed would not predominantly furnished by fossil fuelled power plants [277]. Nevertheless, the consumption of electricity related to MW activation varies a lot and it is reported in the range of 200–40,000 kWh/tonne dried biomass, typically 2500–10,000 kWh(e)/tonne dried biomass, depending on the type of employed feedstock, on the reactor model, on the chemicals used, on the gas atmosphere and operating conditions [278,279]. Such estimation was done by considering lab scale tube reactors or fixed beds employed in batch MW activation and may not be utilized for practical applications. In addition, many studies dealt mainly with the effect of the different parameters and on the characterisation of AC, while disregarding the initial mass of the AC precursor, that would add uncertainty to the consumption of electricity. It was reported that the cost for producing 1 kg of AC by MW heating is US$ 32.43, whereas the cost of 1 kg of AC produced by conventional heating is US$ 70.67, proving that MW heating reduced of > 50 % the cost of the total production of AC [280].

The analysis of the costs related to the production of AC is tightly related to the specific biomass feedstock, to the process configuration and to the plant location. MW heating can be considered as a mature technology. On the other hand, the MW-assisted production of AC at large scale is still distant from maturity even though some pilot and demonstration plants are operating in China and overseas. In this contest, information coming from small-scale reactors would not be helpful for the technology scale up and would not provide the knowledge on the performance of how large-scale MW plants [281]. Finally, undesired pollutants (such as H_2SO_4, HNO_3, KOH, etc.) and unwanted gases (such as SO_2, NO_2, etc.). may be liberated into the environment during the activation and application process. Hence, special attention has to be devoted to a careful evaluation the potential environmental contamination to minim ize the environmental impact and to enhance the stability of activated biochar.

8 Final remarks

The use of dielectric heating technology for waste feedstock valorization offers intriguing future perspectives that go over and beyond the development of a sustainable process for the production high added value products, biofuels and materials. High-throughput applications of MW assisted flash process would entail the use of flow MW reactors. On a broader perspective, MW process intensification will play a crucial role in the industrial realization of a bio-based chemical business instead of petrochemicals.

[1] V.L. Budarin, P.S. Shuttleworth, M.D. Bruyn, T.J. Farmer, M.J. Gronnow, L. Pfaltzgraff, D.J. Macquarrie, J.H. Clark, *Catal. Today*, 2015, **239**, 80-89.
[2] J. Asomaning, S. Haupt, M. Chae, D. C. Bressler, *Renew Sust Energ Rev*, 2018, **92**, *642–657*.
[3] X. Zhang, K. Rajagopalan, H. Lei, R. Ruanc, B K. Sharma, *Sustain. Energy Fuels*, 2017, **1**, 1664–1699.
[4] M. Miura, H. Kaga, A. Sakurai, T. Kakuchi, K. Takahashi, *J. Anal. Appl. Pyrolysis*, 2004, **71**, 187–199.
[5] C. Yin, *Bioresour Technol,* 2012, **120**, 273-284.
[6] D.J. Macquarrie, J.H. Clark, E. Fitzpatrick, *Biofuels Bioprod Bioref*, 2012, **6**, 549–560.
[7] Y.-F. Huang, P.-T. Chiueh, S.-L. Lo, *Sustain Environ. Res*., 2016, **26**, 103-109.
[8] F. Mushtaq, R. Mat, F. N. Ani, *Renew. Sustain. Energy Rev.*, 2014, **39**, 555–574.
[9] J. Asomaning, S. Haupt, M. Chae, D. C. Bressler, *Renew. Sustain. Energy Rev.,* 2018, **92**, 642–657.
[10] K.M. Picker, S.W. Hoag, *J Pharm Sci*, 2002*,* **91**, 342–349.
[11] S. Tabasso, Microwave-assisted biomass conversion. In: Microwave Chemistry, 2017, Cravotto G. (Ed.), Carnaroglio D. (Ed.) De Gruyter Graduate GmbH, Boston, 370-381.
[12] J. Fan, M. De bruyn, V. L. Budarin, M. J. Gronnow, P. S. Shuttleworth, S. Breeden, D. J. Macquarrie, J. H. Clark, *J. Am. Chem. Soc*. 2013, **135**, 11728−11731.
[13] C. Zhaia, N.Tenga, B. Pana, J.Chena, F. Liua, J. Zhua, H. Na, *Carbohydr Polym*. 2018, **197**, 414-421.
[14] V. L. Budarin, P. S. Shuttleworth, M.De bruyn, T. J. Farmer, M. J. Gronnow, L. Pfaltzgraff, D. J. Macquarrie, J. H. Clark, *Catal. Today*, 2015, **239**, 80-89.
[15] S.Pacala, R. Socolow, *Science* 2004, **305**, 968-972.
[16] J. J. Bozell, G. R. Petersen, *Green Chem.* 2010, **12**, 539-554.
[17] L. Cao, C. Zhang, H. Chen, D. Tsang, G. Luo, S. Zhang, J. Chen, *Bioresour. Technol*. 2017, **245**, 1184−1193.
[18] C. L. Chong, Z. Qing, L. Yechun, H. Yihuai, H. Wang, Z. Guichen, *Energy Fuels*, 2018, **32**, 510−516.
[19] X. Huang, F. Li, J. Xie, C. De Hoop, C. Hse, J. Qi, H. Xiao, *Bioresource*, 2017, **12**, 1968-1981.
[20] G. Li, C. Hse, T. Qin, *J Res*, 2015, **26**, 1043–1048.
[21] J. Remón, A. S. Matharu, J.H. Clark, Energy conversion and Management, 2018, **165**, 634-648.
[22] G. Cravotto, D. Carnaroglio Eds. "Microwave Chemistry (De Gruyter Textbook)" De Gruyter; 1 edition 2017
[23] D. Carnaroglio, S. Tabasso, B. Kwasek, D. Bogdal, E. Calcio Gaudino, G. Cravotto, *ChemSusChem* 2015, **8(8)**, 1342-1349.
[24] V. Choudhary, S.H. Mushrif, C. Ho, A. Anderko, V. Nikolakis, N.S. Marinkovic, A.I. Frenkel, S.I. Sandler, D.G. Vlachos, *J. Am. Chem. Soc.* 2013, **135 (10)**, 3997-4006.
[25] Z. Xue, Q. Liu, J. Wang, T. Mu, *Green Chem*., 2018, **20**, 4391-4408.
[26] O. A. Abdelrahman, A. Heyden, J. Q. Bond, *ACS Catal.*,2014, **4**, 1171-1181.
[27] W. Luo, M. Sankar, A. M. Beale, Q. He, C. J. Kiely, P. C. A. Bruijnincx, B. M. Weckhuysen, *Nat. Commun*., 2015, **6**, 6540-7540.
[28] T. Mizugaki, K. Togo, Z. Maeno, T. Mitsudome, K. Jitsukawa, K. Kaneda, *ACS Sustainable Chem. Eng*., 2016, **4**, 682-685.
[29] K. Kon, W. Onodera, K.-i. Shimizu, *Catal. Sci. Technol*., 2014, **4**, 3227-3234.
[30] J. Lv, Z. Rong, L. Sun, C. Liu, A.-H. Lu, Y. Wang, J. Qu, *Catal. Sci. Technol.*, 2018, **8**, 975-979.
[31] I. Podolean, V. Kuncser, N. Gheorghe, D. Macovei, V. I. Parvulescu, S. M. Coman, *Green Chem.*, 2013, **15**, 3077-3082.
[32] J. Zhang, B. Xie, L. Wang, X. Yi, C. Wang, G. Wang, Z. Dai, A. Zheng, F.-S. Xiao, *ChemCatChem*, 2017, **9**, 2661.
[33] H. Heeres, R. Handana, D. Chunai, C. B. Rasrendra, B. Girisuta and H. J. Heeres, *Green Chem*., 2009, **11**, 1247-1255
[34] R. Weingarten, W. C. Conner, G. W. Huber, *Energy Environ. Sci*., 2012,**5**, 7559-7574.
[35] N.A.S. Ramli, N.A.S. Amin, *Appl.Catal. B-Environ*. 2015, 163, 487-498.
[36] J. Y. Cha and M. A. Hanna, Ind. Crop. Prod., 2002, 16, 109-118.
[37] A. Szabolcs, M. Molnár, G. Dibó and L. Mika, Green Chem., 2013, 15, 439-445.
[38] S. Tabasso, E. Montoneri, D. Carnaroglio, M. Caporaso, G. Cravotto, *Green Chem.*, 2014, **16(1)**, 73-76.
[39] V. B. Kumar, I. N. Pulidindi, A. Gedanken, *RSC Advances*, 2015, **5(15)**, 11043-11048.
[40] W. Ronen, Y. T. Kim, G. A. Tompsett, A. Fern´andez, K. S. Han, E. W. Hagaman, W. C. J. Conner, J. A. Dumesic and G. W. Huber, *J. Catal.*, 2013, **304**, 123-134.
[41] M. Francavilla, S. Intini, L. Luchetti, R. Luque, *Green Chem*. 2016, **18(22)**, 5971-5977.
[42] J. M. Tukacs, A. T. Hollo, N. Retfalvi, E. Csefalvay, G. Dibo, D. Havasi, L. T. Mika, *Chem. Select*, 2017, **2(4)**, 1375-1380.
[43] S. Maiti, G. Gallastegui, G. Suresh, V. L. Pachapur, S. K. Brar, Y. Le Bihan, P. Drogui, G. Buelna, M. Verma, R. Galvez-Cloutier, *Biores. Technol*., 2018, **265**, 471-479.
[44] H. Li, Z. Fang, J. Luo and S. Yang, *Appl. Catal., B*, 2017, **200**, 182-191.
[45] L. Yang, X. Yang, E. Tian, V. Vattipalli, W. Fan and H. Lin, *J. Catal*, 2016, **333**, 207-216.
[46] J. Feng, J. Jiang, C. Y. Hse, Z. Yang, K. Wang, J. Ye, J. Xu, *Sust. Energy & Fuels*, 2018, **2(5)**, 1035-1045.

[47] C. O. Tuck, E. Perez, I. T. Horvath, R. A. Sheldon, M. Poliakoff, *Science* 2012, **337**, 695-699.
[48] C. S. M. Pereira, V. M. T. M. Silva, A. E. Rodrigues, Green Chem. 2011, **13**, 2658-2671.
[49] G.-Q. Chen, M. K. Patel, *Chem. Rev*. 2012, **112**, 2082-2099.
[50] N. Wang, X. Shen Wu, C. Li, M. Fang Feng, *J. Biomater. Sci. Polym*. Ed. 2000, **11**, 301-318.
[51] R. Datta, M. Henry, *J. Chem. Technol. Biotechnol*. 2006, **81**, 1119-1129.
[52] D. Carnaroglio, S. Tabasso, B. Kwasek, D. Bogdal, E. Calcio Gaudino, G. Cravotto, *ChemSusChem* 2015, **8(8)**, 1342-1349.
[53] S.P. Dubey, H.A. Abhyankar,V. Marchante, J.L. Brighton, B. Bergmann, G. Trinhc, C. David, *RSC Adv.*, 2017, **7**, 18529-18538.
[54] J. J. Bozell, G. R. Petersen, Green Chem., 2010, **12**, 539-554.
[55] A.S. Dias, S. Lima, M. Pillinger, A.A. Valente, *Carbohydr. Res.* 2006, **341**, 2946-2953.
[56] R. Mariscal, P. Maireles-Torres, M. Ojeda, I. Sadaba and M. Lopez Granados, *Energy Environ. Sci.*, 2016, **9**, 1144-1189.
[57] R. Crossley, P. Schubel, A. Stevenson, *J. Reinf. Plast. Comp.* 2014, **33**, 58-68.
[58] G. Machado, S. Leon, F. Santos, R. Lourega, J. Dullius, M. E. Mollmann, P. Eichler, Nat. Res., 2016, **7**, 115-129.
[59] C. Sanchez, L. Serrano, M. A. Andres, J. Labidi, *Ind. Crops and Prod.*, 2013, **42**, 513-519.
[60] S. Jr Vaz, P. M. Donate, *BioRes.*, 2015, **10(4)**, 8168-8180.
[61] G. Cravotto, D. Carnaroglio Eds. "Microwave Chemistry (De Gruyter Textbook)" De Gruyter; 1 edition 2017
[62] C. Antonetti, E. Bonari, D. Licursi, N. Nassi o Di Nasso, A. M. Galletti Raspolli, Molecules 2015, 20(12), 21232-21253.
[63] J. Ren, W. Wang, Y. Yan, A. Deng, Q. Chen, L. Zhao, Cellulose, 2016, **23(3)**, 1649-1661.
[64] I. Agirrezabal-Telleria, A. Larreategui, J. Requies, M.B. Güemez, P.L. Arias, *Bioresour. Technol*. 2011, **102**, 7478-7485.
[65] O. Yemiş, G. Mazza, Waste and Biomass Valorization, https://doi.org/10.1007/s12649-017-0144-2
[66] L. Liu, J. Sun, M. Li, S. Wang, H. Pei, J. Zhang, *Bioresour. Technol.* 2009, **100**, 5853-5858.
[67] K. De Oliveira Vigier, A. Benguerba, J. Barrault, F. Jerome, *Green Chem*. 2012, **4**, 285-289.
[68] J. Sun, X. Yuan, Y. Shen, Y. Yi, B. Wang, F. Xu, R. Sun, *Ind. Crops Prod*., 2015, **70**, 266-271.
[69] S. Le Guenic, F. Delbecq, C. Ceballos, C. Len, *J. Mol. Catal. A: Chem.* 2015, **410**, 1-7.
[70] F. Delbecq, Y. Wang, C. Len, *J. Mol. Catal. A: Chem*., 2016, **423**, 520-525.
[71] J. R. Weingarten, G. A. Tompsett, W. C. Conner and G. W. Huber, *Green Chem*., 2010, **12**, 1423-1429.
[72] J.-P. Lange, *Angew. Chem., Int. Ed*., 2015, **54**, 13186-13200.
[73] Q. Zhang, K. De Oliveira Vigier, S. Royer and F. Jérôme, *Chem. Soc. Rev*., 2012, **41**, 7108-7146.
[74] S. Jiang, C. Verrier, M. Ahmar, J. Lai, C. Ma, E. Muller, Y. Queneau, M. Pera-Titus, F. Jérômea, K. De Oliveira Vigier, *Green Chem.*, 2018, DOI: 10.1039/c8gc02260g.
[75] I. K. M. Yu, D. C. W. Tsang, A. C. K. Yip, A. J. Hunt, J. Sherwood, J. Shang, H. Song, Y. S. Ok, C. S. Poon, *Green Chem.*, 2018, **20(9)**, 2064-2074.
[76] J. He, M. Liu, K. Huang, T. W. Walker, C. T. Maravelias, J. A. Dumesic and G. W. Huber, *Green Chem*., 2017, **19**, 3642-3653.
[77] S. Tabasso, G. Grillo, D. Carnaroglio, E. Calcio Gaudino, G. Cravotto, *Molecules*, 2016, **21(4)**, 13/1.
[78] V.L. Budarin, P.S. Shuttleworth, M.D. Bruyn, T.J. Farmer, M.J. Gronnow, L. Pfaltzgraff, D.J. Macquarrie, J.H. Clark, *Catal. Today*, 2015, **239**, 80-89
[79] S. S. Lam, R. K. Liew, A. Jusoh, C. T. Chong, F. N. Ani and H. A. Chase, H.A., *Renew. Sust. Energ. Rev.*, 2016, **53**, 741–753.
[80] W. A. Wan Mahari, N. F. Zainuddin, C. T. Chong, C. L. Lee, W. H. Lam, S. C. Poh and S. S., Lam, *J. Environ. Chem. Eng.*, 2017, **5**, 5836–5842.
[81] V. L. Budarin, P. S. Shuttleworth, M. De bruyn, T. J. Farmer, M. J. Gronnow, L. Pfaltzgraff, D. J. Macquarrie, J. H. Clark, *Catal. Today,* 2015, **239**, 80-89.
[82] X. Zhang, K. Rajagopalan, H. Lei, R. Ruan, B. K. Sharma, *Sust. Energy Fuels*, 2017, **1**, 1664-1699.
[83] F. Motasemi, M.T. Afzal, *Renew Sust Energ Rev*., 2013, **28**, 317-330.
[84] G. Visioli, F. D. Conti, C. Menta, M. Bandiera, A. Malcevschi, D. L. Jones and T. Vamerali, *Environ. Monit. Assess.*, 2016, **188**, 1–11.
[85] W. L. Nam, X. Y. Phang, M. H. Su, R. K. Liew, N. L. Ma, M. H. N. B. Rosli and S. S. Lam, *Sci. Total Environ.*, 2018, **624**, 9–16.
[86] R. K. Liew, W. L. Nam, M. Y. Chong, X. Y. Phang, M. H. Su, P. N. Y. Yek, N. L. Ma, C. K. Cheng, C. T. Chong and S. S. Lam, *Process Saf. Environ.*, 2018, **115**, 57–69.
[87] S. S. Lam, R. K. Liew, C. K. Cheng, N. Rasit, C. K. Ooi, N. L. Ma, J.-H. Ng, W.H. Lam, C. T. Chong and H. A. Chase, *J. Environ. Manage.,* 2018, **213**, 400–408.
[88] S. S. Lam, R. K. Liew, C. K. Cheng and H. A. Chase, *Appl. Catal. B Environ.*, 2015, **176**, 601–617.
[89] X. Tan, S. Liu, Y. Liu, Y. Gu, G. Zeng, X. Hu, X. Wang, S. Liu and L. Jiang, *Bioresour. Technol.*, 2017, **227**, 359-372.
[90] D. Chen, X. Chen, J. Sun, Z. Zheng and K. Fu, *Bioresour. Technol.*, 2016, **216**, 629–636.

[91] S. S. Lam, R. K. Liew, Y. M. Wong, N. Y. P. Yek, N. L. Ma, C. L. Lee, H. A. Chase, *J. Clean. Prod.*, 2017, **162**, 1376–1387.
[92] W. A. Wan Mahari, N. F. Zainuddin, W. M. N. Wan Nik, C. T. Chong, and S. S. Lam, *Energies*, 2016, **9**, 780-788.
[93] S. S. Lam, R. K. Liew, Y. M. Wong, E. Azwar, A. Jusoh and R. Wahi, *Waste Biomass Valori.*, 2017, **8**, 2109–2119.
[94] F. Mushtaq, T. A. T. Abdullah, R. Mat and F. N. Ani, *Bioresour. Technol.*, 2015, **190**, 442–450.
[95] Y.F. Huang, P.T. Chiueh, W.H. Kuan, S.L.Lo, *Energy* 2016, **100**, 137-144.
[96] T.J. Appleton, R.I. Colder, S.W. Kingman, I.S. Lowndes, A. G. Read. *Appl Energy,* 2005, **81**, 85-113.
[97] S. Farag, D. Fu, P. G.Jessop, J. Chaouki, *J. Anal. Appl. Pyrolysis*, 2014, **109**, 249-257.
[98] A.A.Shra'ah, R.Helleur, *J. Anal. Appl. Pyrolysis*, 2014, **105**, 91-99.
[99] D.V. Suriapparao, R. Vinu, *RSC Adv.*, 2015, **5**, 57619-57631.
[100] C. Zhao, E. Jiang, A. Chen, *J. Energy Inst.* 2016, **90**, 902-913.
[101] J. Robinson, C. Dodds, A. Stavrinides, S. Kingman, J. Katrib, Z. Wu, J. Medrano, R. Overend, *Energy Fuels,* 2015, **29**, 1701-1709.
[102] P. Shuttleworth, V. Budarin, M. Gronnow, *RSC Green Chem. Series*: *Economic Utilisation of Food Co-Products*, Royal Society of Chemistry, Cambridge, 2013.
[103] J. A. Menéndez, A. Arenillas, B. Fidalgo, Y. Fernández, L. Zubizarreta, E. G. Calvo and J. M. Bermúdez, *Fuel Process. Technol.*, 2010, **91**, 1–8.
[104] D. A. Jones, T. P. Lelyveld, S. D. Mavrofidis, S. W. Kingman and N. J. Miles, *Resour. Conserv. Recy.*, 2002, **34**, 75–90.
[105] E.R. Umeki, C.F de Oliveira, R.B. Torres, R.G.D. Santos, Fuel, 2016, **185**, 236-242.
[106] F. Motasemi, M.T. Afzal, *Renew Sustain Energy Rev*, 2013, **28,** 317.
[107] D.V. Suriapparao, N. Pradeep, R. Vinu, *Energy Fuel*, 2015, **29 (4)**, 2571-2581.
[108] Y.F. Huang, P. Te Chiueh, W.H. Kuan, S.L. Lo., *Bioresour Technol,* 2013, **142**, 620-624.
[109] X. Zhao, M. Wang, H. Liu, C. Zhao, C. Ma, Z. Song, *J. Anal Appl Pyrolysis* 2013, **100**, 49-55.
[110] Y.F. Huang, P. T. Chiueh, W. H., S. L. Lo, *Energy*, 2015, **89**, 974–981.
[111] M.A. Jamaluddin, K. Ismail, M.A. Mohd Ishak, Z. Ab Ghani, M.F. Abdullah, M.T.U. Safian, S.S. Idris, S. Tahiruddin, M.F. Mohammed Yunus, N.I.N. Mohd Hakimi, *Renew Energy*, 2013, **55**, 357–365.
[112] Y.-F. Huang, P.-T. Chiueh, W.-H. Kuan, S.-L. Lo, *Bioresour. Technol.*, 2013, **142**, 620–624.
[113] J. Chaouki, "A Review of Microwave Pyrolysis of Biomass and Waste for the Production of Energy and Fuels" in "BioEnergy IV: Innovations in Biomass Conversion for Heat, Power, Fuels and Chemicals", Manuel Garcia-Perez,Washington State University, USA Dietrich Meier, Thünen Institute of Wood Research, Germany Raffaella Ocone, Heriot-Watt University, United Kingdom Paul de Wild, Biomass & Energy Efficiency, ECN, The Netherlands Eds, ECI Symposium Series, (2013). http://dc.engconfintl.org/bioenergy_iv/30
[114] Z. Abubakar, A.A. Salema, F.N. Ani, *Bioresour Technol*, 2013, **128**, 578–585.
[115] J.E. Omoriyekomwan, A. Tahmasebi, J. Yu, *Bioresour Technol*, 2016, **207**, 188-196.
[116] Y.-F. Huang, P.-T. Chiueh, W.-H. Kuan, S.-L. Lo, *Energy*, 2016, **100**, 137–144.
[117] C. Ravikumar, K. P. Senthil, S.K. Subhashni, P. V. Tejaswini, V. Varshini V. *Sustain Mater Technol*, 2017, **11**, 19–27.
[118] F.C. Borges, Z. Du, Q. Xie, J.O. Trierweiler, Y. Cheng, Y. Wan, Y. Liu, R. Zhu, X. Lin, P. Chen, R. Ruan, *Bioresour Technol*
2014, **156**, 267–274.
[119] Y.-F. Huang, W. H. Kuan, C.-C. Chang, Y.-M. Tzou, *Bioresour Technol*, 2013, **131**, 274–280.
[120] S. Ren, H. Lei, L. Wang, G. Yadavalli, Y. Liu, J. Julson, *J Anal Appl Pyrolysis*, 2014, **108**, 248–253.
[121] B. Zhang, Z. Zhong, Q. Xie, S. Liu, R. Ruan, *J Environ Sci*, 2016, **45**, 240–247.
[122] F. Mushtaq, C.A. Sami, R. Mat, F.N. Ani, *Appl Mech Mater*, 2014, 307–311.
[123] H. Li, X. Li, L. Liu, K. Li, X. Wang, H. Li, *Int J Hydrog Energy*, 2016, **41**, 2263–2267.
[124] Y.C. Lin, T.Y. Wu, W.Y. Liu, Y.H. Hsiao, *Fuel*, 2014, **119**, 21–26.
[125] F. Motasemi, M.T. Afzal, A.A. Salema, J. Mouris, R.M. Hutcheon, *Fuel*, 2014, **124**, 151–157.
[126] B.A. Mohamed, C.S. Kim, N. Ellis, X. Bi, *Bioresour Technol*, 2016, **201**, 121–132.
[127] M. Bartoli, L. Rosi, A. Giovannelli, P. Frediani, M. Frediani M., *J Anal Appl Pyrolysis*, 2016, **122**, 479–489.
[128] R. Zhou, W.H. Lei, J. Julson, *J Anal Appl Pyrolysis*, 2013, **101**, 172-176.
[129] Q. Dong, Y. Xiong, *Bioresour Technol,* 2014, **171**, 127–131.
[130] Z. M.A. Bundhoo, *Renew. Sustain. Energy Rev.*, 2018, **82**, 1149–1177.
[131] Y-F. Huang, P-T. Chiueh, S-L. Lo S-L. *Sustain Environ Res*, 2016, **26**, 103-109.
[132] D.V. Suriapparao, N. Pradeep, R. Vinu, *Energy Fuels*, 2015, **29**, 2571–2581.
[133] H. Shang, R.-R. Lu, L. Shang, W.-H. Zhang, *Fuel Process.Technol.*, 2015, **131**, 167–174.
[134] A. Mamaeva, A. Tahmasebi, L. Tian and J. Yu, *Bioresour. Technol.*, 2016, **211**, 382–389.

[135] P. C. Tarves, C. A. Mullen, A. A. Boateng, *ACS Sustainable Chem. Eng*. 2016, **4**, 930−936.
[136] Y. Wang, Z. Zhou, M. Chen, Y. Huang, C. Wang and W.-L. Song, *Appl. Surf. Sci.*, 2018, **439**, 176–185
[137] O. Baytar, Ö. Şahin and C. Saka, *Appl. Therm. Eng.*, 2018, **138**, 542–551.
[138] S.-H. Ho, C. Zhang, W.-H. Chen, Y. Shen and J.-S. Chang, *Bioresour. Technol.*, 2018, **264**, 7–16.
[139] D. Touhami, Z. Zhu, W. S. Balan, J. Janaun, S. Haywood and S. Zein, *J. Env. Chem. Eng.*, 2017, 5, 2388–2394.
[140] N. Ferrera-Lorenzo, E. Fuente, I. Suárez-Ruiz and B. Ruiz, *Fuel Process. Technol.*, 2014, **121**, 25–31.].
[141] D. V. Suriapparao, N. Pradeep, R. Vinu, *Energy Fuels*, 2015, **29**, 2571–2581.
[142] F. C. Borges, Z. Du, Q. Xie, J. O. Trierweiler, Y. Cheng, Y. Wan, Y. Liu, R. Zhu, X. Lin, P. Chen and R. Ruan, *Bioresour. Technol.*, 2014, **156**, 267–274.
[143] S.P. Zhang, Q. Dong, L. Zhang, Y.Q. Xiong YQ. *Bioresour Technol* 2015, **191**, 17-23.
[144] Q. Bu, H. Lei, L. Wang, G. Yadavalli, Y. Wei, X. Zhang, L. Zhu and Y. Liu, *J. Anal. Appl. Pyrolysis*, 2015, **112**, 74–79.
[145] L. Zhou, Y. Jia, T.-H. Nguyen, A. A. Adesina and Z. Liu, *Fuel Process. Technol.*, 2013, **116**, 149–157.
[146] H. Shang, R.-R. Lu, L. Shang, W.-H. Zhang, *Fuel Process.Technol.*, 2015, **131**, 167–174.
[147] B. A. Mohamed, C. S. Kim, N. Ellis and X. Bi, Bioresour. Technol., 2016, **201**, 121–132.
[148] F. Motasemi, M.T. Afzal, A.A. Salema, J. Mouris, R.M. Hutcheon, *Fuel*, 2014, **124**, 151–157.
[149] Y.-F. Huang, W.-H. Kuan, C.-C. Chang, Y.-M. Tzou, *Bioresour Technol*, 2013, **131**, 274–280.
[150] W.-H. Kuan, Y.-F. Huang, C.-C. Chang, S.-L. Lo, *Bioresour Technol*, 2013, **146**, 324–329.
[151] A. Mamaeva, A. Tahmasebi, L. Tian and J. Yu, *Bioresour. Technol.*, 2016, **211**, 382–389.
[152] X. Zhang, H. Lei, L. Zhu, M. Qian, J. C. Chan, X. Zhu, Y. Liu, G. Yadavalli, D. Yan, L. Wang, Q. Bu, Y. Wei, J. Wu, S. Chen, *Catal. Sci. Technol.*, 2016, **6**, 4210–4220.
[153] H.M. Morgan, H. Marion Jr., Q. Bu, L. Jianghui, L. Yujing, M. Hanping, S. Aiping, L. Hanwu, R. Roger, *Bioresour Technol*, 2017, **230**, 112–121.
[154] Y. Wang, L. Dai, R. Wang, L. Fan, Y. Liu, Q. Xie, R. Ruan, *J. Anal. Appl. Pyrol.*, 2016, **119**, 251–258.
[155] Q. Bu, H.M Morgan, J. Liang, H. Lei, R. Ruan,. Chapter two – catalytic microwave pyrolysis of lignocellulosic biomass for fuels and chemicals. In: Yebo, L., Xumeng, G. (Eds.), Advances in Bioenergy, vol. 1. Elsevier, New York, 2016, 69–123.
[156] X. Z. Xuesong, K. Rajagopalan, H. L. Hanwu, R. Ruan, B. K. Sharma, *Sustain. Energy Fuels*, 2017, **1**, 1664–1699.
[157] X. Zhang, H. Lei, L. Wang, L. Zhu, Y. Wei, Y. Liu, G. Yadavalli, D. Yan, *Green Chem.*, 2015, **17**, 4029–4036.
[158] X. Zhang, H. Lei, L. Zhu, M. Qian, X. Zhu, J. Wu and S. Chen, *Appl. Energy*, 2016, **173**, 418–430.
[159] H. Luo, L-W. Bao, L.Z. Kong, Y.-H Sun, *AIChE* Journal, 2018, **64**, 2124-2134.
[160] E.T. Kostas, D. Beneroso, J.P. Robinson, *Renew Sustain Energy Rev*. 2017, **77**, 12–27.
[161] S. Tabasso, Microwave-assisted biomass conversion. In: Microwave chemistry., Cravotto G. (Ed.), Carnaroglio D. (Ed.), 2017, De Gruyter Graduate GmbH, Boston, 366-378.
[162] V.L. Budarin, P.S. Shuttleworth, M.D. Bruyn, T.J. Farmer, M.J. Gronnow, L. Pfaltzgraff, D.J. Macquarrie, J.H. Clark, *Catal. Today*, 2015, **239**, 80-89
[163] V.L. Budarin, P.S. Shuttleworth, M.D. Bruyn, T.J. Farmer, M.J. Gronnow, L. Pfaltzgraff, D.J. Macquarrie, J.H. Clark, *Catal. Today*, 2015, **239**, 80-89
[164] D.C. Elliott, P. Biller, A.B. Ross, A.J. Schmidt, S.B. Jones, *Bioresour Technol*, 2015, **178**, 147–156.
[165] Z. M.A. Bundhoo, *Renew. Sustain. Energy Rev.*, 2018, **82**, 1149–1177.
[166] S. Nizamuddin, H. A. Baloch, M. T. H. Siddiqui, N. M. Mubarak, M. M. Tunio, A. W. Bhutto, A. S. Jatoi, G. J. Griffin, M. P. Srinivasan, *Rev Environ Sci Biotechnol*, 2018, **17**, 813-837.
[167] S.E. Elaigwu, G.M. Greenway, *Fuel Process Technol*, 2016, **149**, 305–312.
[168] S. Kannan, Y. Gariepy and G. S. V. Raghavan, *Energy Fuels*, 2017, **31**, 4068−4077
[169] S. Kannan, Y. Gariepy and G. S. V. Raghavan, *Waste Management*, 2017, **65**, 159–168
[170] L. Lin, S.-R. Zhai, Z.-Y. Xiao, Y. Song, Q.-D. An and X.-W. Song, *Bioresour. Technol.*, 2013, **136**, 437–443.
[171] S. E. Elaigwu and G. M. Greenway, *Fuel Process. Technol.*, 2016, **149**, 305–312.
[172] S. E. Elaigwu and G. M. Greenway, *J. Anal. Appl. Pyrolysis*, 2016, **118**, 1–8.
[173] W. J. Liu, H. Jiang and H. Q. Yu, *Chem. Rev.*, 2015, **115**, 12251–12285.
[174] X. F. Tan, Y. G. Liu, G. M. Zeng, X. Wang, X. J. Hu, Y. L. Gu and Z. Z. Yang, *Chemosphere*, 2015, **125**, 70–85.
[175] V. Nair and R. Vinu, *Bioresour. Technol.*, 2016, **216**, 511–519.
[176] X. F. Tan, Y. G. Liu, G. M. Zeng, X. Wang, X. J. Hu, Y. L. Gu and Z. Z. Yang, *Chemosphere*, 2015, **125**, 70–85.
[177] M. B. Ahmed, J. L. Zhou, H. H. Ngo and W. Guo, *Biomass Bioenergy*, 2016, **84**, 76–86.
[178] A. U. Rajapaksha, S. S. Chen, D. C. W. Tsang, M. Zhang, M. Vithanage, S. Mandal, B. Gao, N. S. Bolan and Y.S. Ok, *Chemosphere*, 2016, **148**, 276–291.
[179] X. F. Tan, Y. G. Liu, Y. L. Gu, Y. Xu, G. M. Zeng, X. J. Hu, S. B. Liu, X. Wang, S. M. Liu and J. Li, *Bioresour. Technol.*, 2016, **212**, 318–333.

[180] M. B. Ahmed, J. L. Zhou, H. H. Ngo, W. Guo and M. Chen, *Bioresour. Technol.*, 2016, **214**, 836–851.
[181] X. Tan, S. Liu, Y. Liu, Y. Gu, G. Zeng, X. Hu, X. Wang, S. Liu and L. Jiang, *Bioresour. Technol.*, 2017, **227**, 359–372.
[182] R. K. Liew, M. Y. Chong, O. U. Osazuwa, W. L. Nam, X. Y. Phang, M. H. Su, C. K. Cheng, C. T. Chong and S. S. Lam, *Res. Chem. Intermediat.*, 2018, **44**, 3849–3865.
[183] J. Dai, H. Cui and J. R. Grace, *Prog. Energy Combust. Sci.*, 2012, **38**, 716–36.
[184] M. Bartoli, L. Rosi, A. Giovannelli, P. Frediani and M. Frediani, *J. Anal. Appl. Pyrolysis*, 2016, **122**, 479–489.
[185] V. Nair and R. Vinu, *Bioresour. Technol.*, 2016, **216**, 511–519.
[186] L. Cao, I. K. M. Yu, D. C. W. Tsang, S. Zhang, Y. Sik Ok, E. E. Kwon, H. Song and C. Sun Poon, *Bioresour. Technol.*, 2018, **267**, 242–248.
[187] T. Cordero-Lanzac, I. Hita, A. Veloso, J. M. Arandes, J. Rodríguez-Mirasol, J. Bilbao, T., Cordero and P., Castaño, *Chem. Eng. J.*, 2017, **327**, 454–464.
[188] B. Güvenatam, E. H. J. Heeres, E. A. Pidko and E. J. M. Hensen, *Catal. Today*, 2016, **259**, 460–466.
[189] L. Cao, I. K. M. Yu, D. C. W. Tsang, S. Zhang, Y. Sik Ok, E. E. Kwon, H. Song and C. Sun Poon, *Bioresour. Technol.*, 2018, **267**, 242–248.
[190] E. M. Villota, H. Lei, M. Qian, Z. Yang, S. M. A. Villota, Y. Zhang and G. Yadavalli, *ACS Sustainable Chem. Eng.*, 2018, **6**, 1318−1326.
[191] Z. Wan and K. Li, *Chemosphere*, 2018, **194**, 370-380
[192] M. Sevilla, G. A. Ferrero and A. B. Fuertes, *Carbon*, 2017, **114**, 50–58.
[193] S. S. Lam, R. K. Liew, Y. M. Wong, N. Y. P. Yek, N. L. Ma, C. L. Lee and H. A. Chase, *J. Clean. Prod.*, 2017, **162**, 1376–1387.
[194] P. González-García, *Renew. Sustain. Energy Rev.*, 2018, **82**, 1393–1414.
[195] M. Danish and T. Ahmad, *Renew. Sust. Energy Rev.*, 2018, **87**, 1–21.
[196] N. A. Rashidi and S. Yusup, *Chem. Eng. J.*, 2017, **314**, 277–290.
[197] A. M. Abioye and F. N. Ani, *Renew. Sust. Energy Rev.*, 2015, **52**, 1282–1293.
[198] W. Ao, J. Fu, X. Mao, Q. Kang, C. Ran, Y. Liu, H. Zhang, Z. Gao, J. Li, G. Liu and J. Dai, *Renew. Sust. Energy Rev.*, 2018, **92**, 958–979.
[199] X. Tan, S. Liu, Y. Liu, Y. Gu, G. Zeng, X. Hu, X. Wang, S. Liu and L. Jiang, *Bioresour. Technol.*, 2017, **227**, 359–372.
[200] Y.-J. Zhang, Z.-J. Xing, Z.-K. Duan, Li Meng and Y. Wang, *Appl. Surf. Sci.*, 2014, **315**, 279–286.
[201] C. Grima-Olmedo, Á. Ramírez-Gómez, D. Gómez-Limón and C. Clemente-Jul, *Heliyon*, 2016, **2**, 1–18.
[202] S. Işıtan, S. Ceylan, Y. Topcu, C. Hintz, J. Tefft, T. Chellappa, J. Guo and J. L. Goldfarb, *Energy Convers. Manag.*, 2016, **127**, 576–588.
[203] S.-H. Jung and J.-S. Kim, *J. Anal. Appl. Pyrolysis*, 2014, **107**, 116–122.
[204] D. Chen, X. Chen, J. Sun, Z. Zheng and K. Fu, *Bioresour. Technol.*, 2016, **216**, 629–636.
[205] I. M. Lima, D. L. Boykin, K. Thomas Klasson and M. Uchimiya, *Chemosphere*, 2014, **95**, 96–104.
[206] Y.-J. Zhang, Z.-J. Xing, Z.-K. Duan, Li Meng and Y. Wang, *Appl. Surf. Sci.*, 2014, **315**, 279–286.
[207] D. Chen, X. Chen, J. Sun, Z. Zheng and K. Fu, *Bioresour. Technol.*, 2016, **216**, 629–636.
[208] G. Selvaraju and N. K. A. Bakar, *J. Clean. Prod.*, 2017, **141**, 989–999.
[209] D. Angın, T.E. Köse and U. Selengil, *Appl. Surf. Sci.*, 2013, **280**, 705–710.
[210] H. Mao, D. Zhou, Z. Hashisho, S. Wang, H. Chen and H.H. Wang, *BioResources*, 2014, **10**, 809–821.
[211] J. Zhang, J. Liu and R. Liu, *Bioresour. Technol.*, 2015, **176**, 288–291.
[212] L. Zhu, H. Lei, L. Wang, G. Yadavalli, X. Zhang, Y. Wei, Y. Liu, D. Yan, S. Chen and B. Ahring, *J. Anal. Appl. Pyrolysis*, 2015, **115**, 149–156.
[213] H.P. Boehm, *Carbon*, 2002, **40**, 145–149.
[214] R. K. Liew, E. Azwar, P. N. Y. Yek, X. Y. Lim, C. K. Cheng, J.-H. Ng, A. Jusoh, W. H. Lam, M. D. Ibrahim, N. L. Ma and S. S. Lam, *Bioresour. Technol.*, 2018, **266**, 1-10.
[215] R. Seaman and J. Seals, *J. Microwave Power EE*, 1991, **26**, 72–81.
[216] A. Zubrik, M. Matik, M. Lovás, K. Štefušová, Z. Danková, S. Hredzák, M. Václavíková, F. Bendek, J. Briančin, L. Machala and J. Pechoušek, *Carbon Letters*, 2018, **26**, 31-42.
[217] M.N. Noraini, E. C. Abdullah, R. Othman and N. M. Mubarak, *Materials Letters*, 2016, **184**, 315–319.
[218] J. A. Menéndez, E. J. Juárez-Pérez, E. Ruisánchez, J. M. Bermúdez and A. Arenillas, *Carbon*, 2011, **49**, 346–349.
[219] B.R. Reddy and R. Vinu, *Fuel Process. Technol.*, 2016, **154**, 96–103.
[220] B. Debalina, R. B. Reddy and R. Vinu, *J. Anal. Appl. Pyrolysis*, 2017, **124**, 310–318.
[221] H. R. Hoseinzadeh, A. Arami-Niya, W. W. M. A. Daud and J. Sahu, *J. Anal. Appl. Pyrolysis*, 2013, **104**, 176–184.
[222] A. Özhan, Ö. S_ahin, M.M. Küçük and C. Saka, *Cellulose*, 2014, **21**, 2457–2467.
[223] P. S. Thue, E. C. Lima, J. M. Sieliechi, C. Saucier, S. L. P. Dias, J. C. P. Vaghetti, F. S. Rodembusch and F. A. Pavan, *J. Coll. Interf. Sci.*, 2017, **486**, 163–175.
[224] M. Sevilla and R. Mokaya, *Energy Environ. Sci.*, 2014, **7**, 1250–1280.
[225] G. Wang, S. Chen, X. Quan, H. Yu and Y. Zhang, *Carbon*, 2017, **115**, 730–739.

[226] G. Singh, I. Y. Kim, K. S. Lakhi, P. Srivastava, R. Naidu and A. Vinu, *Carbon*, 2017, **116**, 448–455.
[227] R. K. Liew, E. Azwar, P. N. Y. Yek, X. Y. Lim, C. K. Cheng, J.-H. Ng, A. Jusoh, W. H. Lam, M. D. Ibrahim, N. L. Ma and S. S. Lam, Bioresour. Technol., 2018, 266, 1-10.
[228] D. Chen, X. Chen, J. Sun, Z. Zheng and K. Fu, *Bioresour. Technol.*, 2016, **216**, 629–636.
[229] M. A. Yahya, Z. Al-Qodah and C. Z. Ngah, *Renew. Sustain. Energy Rev.*, 2015, **46**, 218–235.
[230] F. Mechati, C. Bouchelta, M. Salah Medjram, R. Benrabaa and N. Ammouchi, *J. Env. Chem. Eng.*, 2015, **3**, 1928–1938.
[231] J. Kazmierczak-Razna and R. Pietrzak, *Adsorption*, 2016, **22**, 473–480.
[232] R. Hoseinzadeh Hesas, A. Arami-Niya, W. M. A. Wan Daud and J. N. Sahu, *J. Ind. Eng. Chem.*, 2015, **24**, 196–205.
[233] I. I. G. Inal, S. M. Holmes, E. Yagmur, N. Ermumcu, A. Banford and Z. Aktas, *J. Ind. Eng. Chem.*, 2018, **61**, 124–132.
[234] T. M. Alslaibi, I. Abustan, M. Azmier Ahmad and A. Abu Foul, *AIChE Journal*, 2014, **60**, 237-250.
[235] A. B. Namazi, D. Grant Allen and C. Q. Jia, *Biomass Bioenergy*, 2015, **73**, 217-224.
[236] M. Bartoli, L. Rosi, A. Giovannelli, P. Frediani, M. Passaponti and M. Frediani, *J. Anal. Appl. Pyrolysis*, 2018, **130**, 305–313.
[237] J. Liang, T. Qu, X. Kun, Y. Zhang, S. Chen, Y.-C. Cao, M. Xie and X. Guo, *Appl. Surf. Sci.*, 2018, **436**, 934–940.
[238] G. Duran Jimenez, T. Monti, J. J. Titman, V. Hernandez-Montoya, S. W. Kingman and E. R. Binner, *J. Anal. Appl. Pyrolysis,* 2017, **124**, 113–121.
[239] T. R. Brazil, M. S.O. Junior, M. R. Baldan, M. Massi and M. C. Rezend, *Vib. Spectrosc.*, 2018, **99**, 130–136.
[240] K. Shi, J. Yan, E. Lester and T. Wu, *Ind. Eng. Chem. Res.*, 2014, **53**, 15012−15019.
[241] Z. Bi, T. Li, H. Su, Y. Ni and L. Yan, *ACS Sustainable Chem. Eng.*, 2018, **6**, 9314−9323.
[242] R. Liu, J. Zhang, M. Gao, Z. Li, J. Chen, D. Wu and P. Liu, *RSC Adv.*, 2015, **5**, 4428-4433.
[243] N. B. Erdal, K. H. Adolfsson, T. Pettersson and M. Hakkarainen, *ACS Sustainable Chem. Eng.*, 2018, **6**, 1246 − 1255.
[244] I. Asomaning, S. Haupt, M. Chae, D. C. Bressler, *Renew Sust Energ Rev*, 2018, **92**, *642–657*.
[245] L. Wang, H. Lei, R. Ruan, Techno-economicanalysis of microwave-assisted pyrolysis for production of biofuels. In: Prod. Biofuels chem. with microw, Fang Z, Smith Jr.RL, Qi X, editors, 2015, Springer, Berlin, 251–64.
[246] J. Robinson, C. Dodds, A. Stavrinides, S. Kingman, J. Katrib, Z. Wu, J. Medrano and R. Overend, *Energy Fuels*, 2015, **29**, 1701–1709.
[247] M. Bhattacharya, T. Basak, *Energy*, 2016, **97**, 306–338.
[248] Q. Bu, H. M. Morgan Jr, J. Liang, H. Lei, R. Ruan, *Advances in Bioenergy*, 2016, **1**, 69–123.
[249] D. Beneroso, T. Monti, E. T. Kostas, J. Robinson, *Chem. Eng. J.*, 2017, **316**, 481–498.
[250] L. Wang, H. Lei, R. Ruan, Techno-economicanalysis of microwave-assisted pyrolysis for production of biofuels. In: Prod. Biofuels chem. with microw, Fang Z, Smith Jr.RL, Qi X, editors, 2015, Springer, Berlin, 251–64.
[251] S. W. Hasan and F. N. Ani, *Ind. Eng. Chem. Res.*, 2014, **53**, 12185−12191
[252] TechSci Research, Global Activated Carbon Market by Type (Powdered Activated Carbon, Granular Activated Carbon and Others), by Raw Material (wood, Coconut Shells, Coal and Others), by Application, Competition Forecast and Opportunities, (2016), pp. 2011–2021 https://www.techsciresearch.com/news/1203-activatedcarbon-market-size-set-to-cross-4-9-billion-by-2021.html, Accessed date: 05 November 2018.
[253] Q. H. Lin, H. Cheng and G. Y. Chen, *J. Anal. Appl. Pyrolysis*, 2012, **93**, 113−119.
[254] Y. Pianroj, S. Jumrat, W. Werapun, S. Karrila and C. Tongurai, *Chem. Eng. Process.*, 2016, **106**, 42–49.
[255] F. L. Braghiroli, H. Bouafif, N. Hamza, B. Bouslimi, C. M. Neculit and A. Koubaa, *Biomass Bioenergy*, 2018, **118**, 105–114.
[256] D. Stefanidis Georgios, N. Muñoz Alexander, S. J. Sturm Guido and A. Stankiewicz, *Rev. Chem. Eng.*, 2014, **30**, 233-259.
[257] Y. Pianroj, S. Jumrat, W. Werapun, S. Karrila and C. Tongurai, *Chem. Eng. Process.*, 2016, **106**, 42–49.
[258] H. Zhang, Z. Gao, W. Ao, J. Li, G. Liu, J. Fu, C. Ran, X. Mao, Q. Kang, Y. Liu and J. Dai, *J. Hazard. Mater.*, 2017, **334**, 112–20.
[259] W. Ao, J. Fu, X. Mao, Q. Kang, C. Ran, Y. Liu, H. Zhang, Z. Gao, J. Li, G. Liu and J. Dai, *Renew. Sustain. Energy Rev.*, 2018, **92**, 958–979.
[260] J. Li, J. Dai, G. Liu, H. Zhang, Z. Gao, J. Fu, Y. He and Y. Huang, *Biomass Bioenergy*, 2016, **94**, 228–244.
[261] W. Ao, J. Fu, X. Mao, Q. Kang, C. Ran, Y. Liu, H. Zhang, Z. Gao, J. Li, G. Liu and J. Dai, *Renew. Sustain. Energy Rev.*, 2018, **92**, 958–979.
[262] F. L. Braghiroli, H. Bouafif, N. Hamza, B. Bouslimi, C. M. Neculit and A. Koubaa, *Biomass Bioenergy*, 2018, **118**, 105–114.
[263] F. L. Braghiroli, H. Bouafif, N. Hamza, B. Bouslimi, C. M. Neculit and A. Koubaa, *Biomass Bioenergy*, 2018, **118**, 105–114.
[264] K. Tan, S. Liu, Y. Liu, Y. Gu, G. Zeng, X. Hu, X. Wang, S. Liu, L. Jiang, *Bioresour. Technol.*, 2017, **227**, 359-372.
[265] S. Ramasamy and B. Moghtaderi, *Energy Fuels*, 2010, **24**, 4534–4548.

[266] K. Y. Foo and B. H. Hameed, *Bioresour. Technol.*, 2013, **130**, 696−702.
[267] K. Y. Foo, L. K. Lee and B. H. Hameed, *Bioresour. Technol.*, 2013, **134**, 166−172.
[268] K. Y. Foo, L. K. Lee and B. H. Hameed, *Bioresour. Technol.*, 2013, **133**, 599−605.
[269] Q.-S. Liu, T. Zheng N., Li, P. Wang and G.Abulikemu, *Appl. Surf. Sci.*, 2010, **256**, 3309−3315.
[270] Z. Abubakar, A. A. Salema and F. N. A Ani, *Bioresour. Technol.*, 2013, **128**, 578−585.
[271] https://ec.europa.eu/eurostat/documents/3217494/5695820/KS-CD-07-001-11-EN.PDF/2b64284f-c7f9-4ed0-bf87-44d70db33b57?version=1.0.
[272] C. Dorn, R. Behrend, D. Giannopoulos, L. Napolano, B. García Baños, V. James, V. Uhlig, J. M. Catalá, M. Founti and D. Trimis, *Procedia CIRP*, 2015, **29**, 492–497.
[273] ISO 14040. Environmental management - Life cycle assessment -Principles and framework, 2006.
[274] ISO 14044. Environmental management - Life cycle assessment -Requirements and guidelines, 2006.
[275] SETAC – Society of Environmental Toxicology and Chemistry, Guidelines for Life Cycle Assessment: A "Code of Practice", SETAC, 1993.
[276] U.S. Environmental Protection Agency and Science Applications International Corporation. LCAccess – LCA 101, EPA, 2001.
[277] C. Dorn, R. Behrend, D. Giannopoulos, L. Napolano, B. García Baños, V. James, V. Uhlig, J. M. Catalá, M. Founti and D. Trimis, *Procedia CIRP*, 2015, **29**, 492–497.
[278] J. Georgin, G. L. Dotto, M. A. Mazutti and E. L. Foletto, *J. Environ. Chem. Eng.*, 2016, **4**, 266–75.
[279] R. Hoseinzadeh Hesas, A. Arami-Niya, W. M. A. Wan Daud and J. N. Sahu, *J. Ind. Eng. Chem.*, 2014, **24**, 196–205.
[280] M. J. Puchana-Rosero, M. A. Adebayo, E. C. Lima, F. M. Machado, P. S. Thue, J. C. P. Vaghetti, C. S. Umpierres and M. Gutterres, *Colloids Surf. A Physicochem. Eng. Asp.*, 2016, **504**, 105–15.
[281] K. Tan, S. Liu, Y. Liu, Y. Gu, G. Zeng, X. Hu, X. Wang, S. Liu, L. Jiang, *Bioresource Technology*, 2017, **227**, 359-372.